Protease activities of vaginal *Porphyromonas* species disrupt coagulation and extracellular matrix in the cervicovaginal niche

Karen V. Lithgow[1], Vienna C.H. Buchholz[1*], Emily Ku[1], Shaelen Konschuh[1], Ana D'Aubeterre[1†], and Laura K. Sycuro[1,2,3,4,#]

[1]Department of Microbiology, Immunology and Infectious Diseases, University of Calgary, Calgary, AB, Canada

[2]Snyder Institute for Chronic Diseases, University of Calgary, Calgary, AB, Canada

[3]Alberta Children's Hospital Research Institute, University of Calgary, Calgary, AB, Canada

[4]International Microbiome Centre, University of Calgary, Calgary, AB, Canada

#Corresponding author: Laura Sycuro, laura.sycuro@ucalgary.ca

*Present affiliation:

Faculty of Medicine & Dentistry, University of Alberta, Edmonton, AB, Canada

[†]Present affiliation:

Department of Biological Sciences, University of Alberta, Edmonton, AB, Canada

Running Title: Protease activity of vaginal *Porphyromonas* species

Abstract: 240 words

Importance: 141 words

Main Text: 7540 words

Abstract

Porphyromonas asaccahrolytica and *Porphyromonas uenonis* are frequently isolated from the human vagina and are linked to bacterial vaginosis and preterm labour. However, little is known about the pathogenesis mechanisms of these bacteria. The related oral opportunistic pathogen, *Porphyromonas gingivalis,* is comparatively well-studied and known to secrete numerous extracellular matrix-targeting proteases. Among these are the gingipain family of cysteine proteases that drive periodontal disease progression and hematogenic transmission to the placenta. Given their phylogenetic relatedness, we hypothesized that vaginal *Porphyromonas* species possess gingipain-like protease activity targeting host extracellular matrix in the female reproductive tract. In this study, we demonstrate that vaginal *Porphyromonas* species degrade type I collagen (cervix), type IV collagen (chorioamnion/placenta), and fibrinogen, but not through the activity of gingipain orthologs. Bioinformatic queries identified 5 candidate collagenases in each species, including serine, cysteine and metalloproteases, with signal peptides directing them to the extracellular environment. Inhibition assays revealed both species secrete metalloproteases that degrade collagen and casein, while *P. asaccharolytica* also secretes a metalloprotease that degrades fibrinogen. Phylogenetic analysis of the predicted collagen-degrading metalloprotease revealed an orthologous relationship with the *P. gingivalis* endopeptidase PepO. Cloning and expression of *P. asaccharolytica* PepO confirmed this protein's collagenase and caseinase activities, which have not previously been attributed to PepO homologs in other bacteria. Altogether, this description of the first known virulence factor in *Porphyromonas* species colonizing the human vagina sheds light on their potential to alter the structural integrity and homeostasis of reproductive tissues.

Importance

Porphyromonas species are common inhabitants of the vaginal microbiome, but their presence has been liked to adverse health outcomes for women, including bacterial vaginosis and preterm birth. We determined that *P. asaccharolytica* and *P. uenonis* secrete broad-acting proteases capable of freely diffusing within the cervicovaginal niche and degrading important components of host tissues, namely the extracellular matrix. We show that secreted *Porphyromonas* proteases degrade collagens that are enriched within the cervix (type I) and chorioamniotic membranes (type IV). Furthermore, these *Porphyromonas* proteases can also degrade fibrinogen and inhibit clot formation. These activities can be partially attributed to a metalloprotease that exhibits broad-acting protease activity and is distantly related to the *P. gingivalis* endopeptidase PepO. This initial characterization of virulence activities in vaginal *Porphyromonas* species highlights their potential to harm human pregnancy through clotting disruption, fetal membrane weakening, and premature cervical remodeling.

Introduction

The vaginal microbiome of healthy reproductive-age women is typically characterized by low species diversity, with *Lactobacillus* dominating the vaginal and ectocervical niches of the lower genital tract (1, 2). A community shift towards high species diversity, with overgrowth of anaerobic bacteria, is associated with increased risk of bacterial vaginosis (BV) (2, 3), acquisition and transmission of sexually transmitted infections (4-6), preterm birth (7-9), and cervical cancer (10-12). Intriguingly, some women harbouring a diverse cervicovaginal microbiome are healthy and asymptomatic (2), suggesting a need to untangle how specific species contribute to poor outcomes. Among BV-associated bacteria, Gram-negative anaerobic rods corresponding to *Prevotella* and black-pigmented *Porphyromonas* species are frequently detected in vaginal samples and significantly associated with the *Bacteroides* morphotype from Nugent scoring (13). While *Prevotella* is an abundant, species-rich and relatively well-studied vaginal clade, comparatively little is known about *Porphyromonas* species inhabiting the human vagina. No *Porphyromonas* species is currently thought to be specific to the human urogenital tract, but *P. asaccharolytica*, *P. uenonis, P. bennonis* and *P. somerae* (in decreasing order of cervicovaginal microbiome citation frequency) exhibit a preference for these niches (3, 14, 15). *P. asaccharolytica* and *P. uenonis* colonize the vagina in 15–50% of healthy women and although their prevalence and abundance increases with BV, they are typically considered low abundance taxa (13, 16-20). Recent studies show these species are predictors of spontaneous preterm labour (9, 21), pelvic inflammatory disease (22, 23), human papillomavirus (HPV) infections progressing to cervical neoplasia (24, 25), and uterine cancer (26, 27). Thus, an improved understanding of the functional capacity of vaginal *Porphyromonas* species is needed.

To date, the only *Porphyromonas* species that has been well-characterized is *P. gingivalis*, a low abundance species in the oral microbiome of both healthy patients and those with gingivitis (28, 29). As a keystone species driving oral (plaque) biofilm formation and periodontal disease progression (30, 31), *P. gingivalis* contributes to local tissue destruction directly and indirectly through the induction of inflammatory processes (32, 33). *P. gingivalis* can also disseminate via the bloodstream to distal infection sites such as the endocardium and joints (34, 35). During pregnancy, *P. gingivalis* has been

105 isolated from the placenta and amniotic fluid of women who delivered preterm (36-38), and in mouse
106 infection models, *P. gingivalis* induces preterm labour via inflammatory activation of the chorioamniotic
107 membranes (34, 39, 40). Pathogenesis mechanisms contributing to these outcomes include a wide
108 array of proteolytic activities carried out by numerous secreted proteases. Among these are the
109 gingipain family of cysteine proteases that drive periodontal disease progression (41), hematogenic
110 transmission to the placenta (29, 40, 42, 43) and preterm labour induction in mice (40). The gingipains
111 degrade many extracellular matrix components, including collagen (44, 45), and amplify their effects by
112 activating and upregulating host matrix metalloproteases (MMPs) that also degrade collagen (46, 47).
113 Furthermore, gingipains can degrade immune factors including immunoglobulins (44, 48), complement
114 components (49, 50), cytokines (51, 52), clotting factors (53, 54), and antimicrobial peptides (55), giving
115 rise to a favourable immune environment for *P. gingivalis* colonization.

116 Proteolytic activity has been previously detected in vaginal fluid from patients with BV (56-58)
117 and characterized in clinical isolates of BV-associated bacteria (59, 60). In fact, collagenase
118 (gelatinase) and caseinase activity of *P. asaccharolytica* (formerly *Bacteroides asaccharolyticus*) was
119 previously reported in screens of *Bacteroides* species detected in human infections (61) and clinical
120 isolates from reproductive tract infections (60). However, further characterization of the enzymes
121 responsible was not conducted, and proteolytic activity of *P. uenonis* has yet to be explored. Given their
122 phylogenetic relatedness and epidemiological similarity, exhibiting high prevalence, low abundance and
123 association with disease, we sought to determine whether vaginal *Porphyromonas* species possess the
124 broad-acting proteolytic virulence activity of *P. gingivalis*. In this study we show that *P. asaccharolytica*
125 and *P. uenonis* are both capable of degrading several extracellular matrix components found within the
126 female genital tract. Our study furthermore reveals differences between the species, suggesting
127 preterm birth-associated *P. asaccharolytica* may secrete more enzymes that contribute collagenase
128 activity. Finally, we report the first virulence factor identified and functionally characterized in *P.*
129 *asaccharolytica* – a metalloprotease that is highly conserved in *P. uenonis* and more distantly related to
130 to the PepO endopeptidase in *P. gingivalis* and other *Porphyromonas* species (62, 63). We

demonstrate this protein exhibits broad-acting proteolytic capacity, which may make it a key microbial virulence factor in the pathogenesis of reproductive health conditions and gynecological cancers.

158 **Materials & Methods**

159 **Bacterial Strains and Growth Conditions.** *Porphyromonas asaccharolytica* CCUG 7834 (type strain,
160 identical to DSM 20707, ATCC 25260 and JCM 6326), *Porphyromonas uenonis* CCUG 48615 (type
161 strain, identical to DSM 23387, ATCC BAA-906 and JCM 13868), *Porphyromonas gingivalis* W50
162 ATCC 53978 and *Lactobacillus crispatus* CCUG 42897 were cultured anaerobically on 1.5% brucella
163 agar (BD Biosciences, Franklin Lakes, MD) supplemented with 5% defibrinated sheep's blood (Dalynn
164 Biologicals, Calgary, AB). For liquid cultivation, supplemented brain heart infusion (sBHI) was prepared
165 by supplementing BHI (BD) with 2% gelatin (BD), 1% yeast extract (ThermoFisher Scientific, Burnaby,
166 BC), 0.8% dextrose (BD) and 0.1% starch (ThermoFisher). Solid and liquid cultivation was conducted
167 at 37°C in an AS-580 anaerobic chamber (Anaerobe Systems, Morgan Hill, CA). Bacterial suspensions
168 were prepared by harvesting cells from solid medium after growth for 16-24 hours (*P. gingivalis, L.*
169 *crispatus*) or 36-48 hours (*P. asaccharolytica*, *P. uenonis)* and resuspending cells in sBHI, sBHI (no
170 gelatin), BHI (no supplements) or PBS. Optical density at 600 nm (OD600) of bacterial suspensions
171 was measured with a Genesys 300 visible spectrophotometer (ThermoFisher Burnaby, BC) and colony
172 forming units per mL (cfu/mL) was calculated using empirically determined cfu/mL/OD600nm for each
173 strain. Serial dilution spot plating was used to verify the cfu/mL of the starting suspensions. Cell-free
174 supernatants (SNs) were harvested during late-log to early stationary phase for each species (*P.*
175 *asaccharolytica* OD600 1.3-1.8; *P. uenonis* OD600 0.8-1.2). Liquid cultures were centrifuged at 10,000
176 × g for 10 minutes at room temperature before the supernatant was filter sterilized (0.2 µm; Pall
177 Laboratory, Mississauga, ON) and stored at -20°C.
178
179 **Collagenase Assays.** Cell suspensions or cell-free supernatants were tested for collagenase activity
180 with the EnzChek Gelatinase/Collagenase assay kit (Invitrogen, Carlsbad, CA) using fluorescein-
181 labelled DQ™ gelatin conjugate (type I collagen, Invitrogen) or a type IV DQ™ collagen conjugate from
182 human placenta (Invitrogen). Reactions were prepared in technical triplicate or quadruplicate by mixing
183 20 µL of substrate at 0.25 mg/mL with 80 µL of reaction buffer and 100 µL of bacterial suspension, cell-
184 free supernatant or media in black optical bottom 96-well plates (Greiner Bio-One, Monroe, NC). Using

a Synergy H1 microplate reader (BioTek, Winooski, VT), plates were incubated at 37°C in atmospheric conditions. Kinetic fluorescence reads were measured at 485 nm excitation/527 nm emission every three minutes over two hours, or every thirty minutes over eighteen hours, for cell suspension and cell-free supernatant assays, respectively. Prior to fluorescence reads, plates were shaken for seven seconds. The mean fluorescence readings of the negative control (substrate in sBHI media) were subtracted from experimental wells and relative fluorescence units (RFU) was plotted over time, with negative values adjusted to zero.

Zymography. The total protein content of *Porphyromonas* cell-free supernatants was determined using a bicinchoninic acid microplate assay (BCA; Pierce, Rockford, IL). Cell-free supernatants were diluted to 8 mg/mL and 5 µL of sample was combined with 5 µL of Novex™ Tris-Glycine SDS Sample Buffer (Invitrogen) to load 40 µg per well. Samples were separated on Novex™ 10% Zymogram Plus (Gelatin; Invitrogen) protein gels at a constant voltage of 125 V in Novex™ 1X Tris-Glycine Running Buffer (Invitrogen). After separation, gels were incubated in Novex™ 1X Renaturing Buffer for 30 minutes at room temperature with gentle agitation, followed by two consecutive incubations in Novex™ 1X Developing Buffer: room temperature for 30 minutes and 37°C for 16 hours. Gels were then stained in Coomassie brilliant blue R-250 solution (Fisher Scientific) and de-stained in 5% (vol/vol) methanol/7.5% (vol/vol) acetic acid in distilled water.

Caseinase Assay. *Porphyromonas* cell-free supernatants were tested for general protease activity using fluorescein-labelled casein (FITC-Casein, ThermoFisher) as a substrate. Reactions were prepared in technical triplicate by mixing 20 µL of substrate at 50 µg/mL with 80 µL of Tris-buffered saline and 100 µL of cell-free supernatant in black optical bottom 96-well plates (Greiner Bio-One). Fluorescence plate reader measurements were performed as described above by measuring 485 nm excitation/527 nm emission every ten minutes over five hours.

Casein Plate Assay. Casein plates were prepared by autoclaving three solutions: 30 g/L instant skim milk power (Pacific Dairy), 19 g/L brain heart infusion (BHI, BD Biosciences) and 30 g/L agar (Fisher Scientific). The solutions were combined in equal volume and 10 mL was added to 100x15 mm petri dishes (Fisher Scientific) to solidify at room temperature. Bacterial suspensions were prepared in PBS and 5 µL was spotted onto casein agar plates. Zones of clearance were measured for each spot after incubating the plates at 37°C under anaerobic conditions for three to six days.

Clotting Assays. Bacterial strains were harvested from solid medium and suspended in 13 mM sodium citrate. Suspensions were centrifuged at 10,000 × g for 7 minutes at room temperature and resuspended in 13 mM sodium citrate. Duplicate cell suspensions, or cell-free controls, were incubated with 50 µL of sterile filtered bovine plasma (Quad Five, Ryegate, MT) for 30 minutes at 37°C under anaerobic conditions. After incubation, samples were blinded and centrifuged at 10,000 × g for seven minutes at room temperature, and 50 µL of HEMOCLOT thrombin time reagent (Hyphen Biomed, Neuville-sur-Oise, France) was added to each reaction. The clotting time for each sample was estimated using a stereo microscope to directly visualize clot formation, indicated by the presence of white precipitate, tendril formation or increased viscosity of the samples. The clotting time for samples that did not form visible clots was recorded as 1800 seconds. To further evaluate final clot size, samples were transferred to a clear 96-well plate and OD (405 nm) was measured for the entire well using the well area scan feature of the Synergy H1 microplate reader (BioTek). The average OD405 nm for each well was blanked against duplicate thrombin-free controls for each experimental sample type.

Fibrinogen Degradation Assay. *Porphyromonas* cell suspensions (10^7 cfu/reaction), sBHI media controls or *Porphyromonas* cell-free supernatants (240 µg of total protein) were incubated with 120 µg of human fibrinogen (Sigma-Aldrich, St. Louis, MO). Reaction mixtures were incubated at 37°C under anaerobic conditions or in an atmosphere of 5% CO_2 for cell suspension or cell-free supernatants, respectively. Samples from each time point (cell suspensions: 0, 2, 18, 24 hours; supernatants: 0, 2, 24, 48 hours) were collected, mixed 1:1 with Novex™ 2X sample buffer (Invitrogen) with dithiothreitol

(DTT, Fisher Scientific), heated at 95°C for 10 minutes and separated on Novex™ 10% Tris-Glycine polyacrylamide pre-cast gels (Invitrogen) at a constant voltage of 180 V. Gels were stained in Coomassie brilliant blue R-250 (0.25% w/v) solution (Fisher Scientific) and de-stained in 5% (vol/vol) methanol/7.5% (vol/vol) acetic acid in H_2O. Fibrinogen degradation was evaluated qualitatively by visualization of fibrinogen α chain (63.5 kDa), β chain (56 kDa) and γ chain (47 kDa) between experimental and control samples over the time-course.

Protease Inhibition Assays. Protease inhibitors were incorporated into collagenase, caseinase and fibrinogen degradation assays, and working solutions were prepared in reaction buffer or TBS. The metalloprotease inhibitor, 1,10-Phenanthroline (Invitrogen), was prepared as a 2 M stock solution in ethanol and diluted to working concentrations of 0.2, 0.02 or 0.002 mM. Iodoacetamide (G-Biosciences, St. Louis, MO, or Sigma-Aldrich) was prepared as a 10 mM stock solution in HyPure H_2O (Cytiva Life Sciences, Marlborough, MA) and used at working concentrations of 0.4, 0.04 or 0.004 mM to inhibit cysteine protease activity. The serine protease inhibitor, aprotinin (Roche, Mississauga, ON) was prepared as a 0.1 mM stock solution in HyPure H_2O (Cytiva Life Sciences) and used at working concentrations of 0.01, 0.001 or 0.0001 mM.

Bioinformatic Analyses. *Gingipain Ortholog Queries.* Gingipain amino acid sequences (RgpA (PGN_1970; P28784), RgpB (PGN_1466; P95493) and Kgp (PGN_1728; B2RLK2) were obtained from *Porphyromonas gingivalis* ATCC 33277 through UniProtKB. Each sequence was queried against all available *P. asaccharolytica* (DSM 20707; PR426713P-I) and *P. uenonis* (DSM 23387; 60-3) genomes using the 'Selected Genomes' protein Basic Local Alignment Search Tool (BLAST; default settings) in the IMG/MER database to identify potential orthologs (Supplemental Figure 1A). Each gingipain AA sequence was also submitted to the Pfam database and all Pfam IDs and names were recorded. Gingipain Pfam IDs were searched against all available *P. asaccharolytica* (DSM 20707; PR426713P-I) and *P. uenonis* (DSM 23387 [IMG Genome ID 2585427891 and 2528311143]; 60-3) strains using the advanced gene search function in the IMG/MER database (Supplemental Figure 5A). All sequences

265 returned by these IMG/MER BLAST and Pfam ID searches were used to query *P. gingivalis* ATCC
266 33277 in a reciprocal BLAST search with the National Center for Biotechnology Information (NCBI)
267 protein BLAST tool (Supplemental Figure 1A). Select hits were aligned with the *P. gingivalis* gingipains
268 across their full length using the EMBL-EMI Clustal Omega alignment tool (64).
269
270 *Candidate Collagenase Queries*. Peptidases from *P. asaccharolytica* CCUG 7834 and *P. uenonis* 60-3
271 were identified by searching for entries with MEROPS peptidase annotations in UniProt (65). For the
272 microbial peptidases from *P. asaccharolytica* and *P. uenonis*, the following enzyme information was
273 exported from UniProtKB for each entry: gene ontology (biological process and molecular function),
274 MEROPs, Pfam, PANTHER, PROSITE, SMART, SUPFAM. Next, a microbial collagenase enzyme
275 number (EC3.4.24.3) was identified in BRENDA (66) and searched against the UniProtKB database
276 (67), generating a list of 3417 entries corresponding to predicted and confirmed microbial collagenases.
277 These microbial collagenase identifiers were cross-referenced against the exported peptidase
278 information from *P. asaccharolytica* and *P. uenonis* to generate a short-list of 14–18 candidate
279 collagenases in *P. asaccharolytica* and *P. uenonis* (Supplemental Figure 1B). Short-list candidates
280 were explored in UniProt and InterPro Scan (68) to eliminate any proteins involved in cell wall synthesis
281 or export machinery and identify the most promising candidates. Sequences were evaluated for the
282 presence of secretion signals using SignalP v.5.0 (69) or integrated information in InterPro. Presence of
283 the IDs: TIGR0483, IPR026444, or PF18962 from TIGR Fam, InterPro and Pfam, respectively, within
284 protein C-termini was indicative of secretion via the type IX secretion system. Since the MEROPs
285 peptidase database only contained information for *P. uenonis* 60-3, IMG BLAST searches were used to
286 identify the corresponding candidate collagenase in the experimental strain used in this study, *P.*
287 *uenonis* CCUG 48615. Sequence identity and InterPro scans were evaluated for the top hit from each
288 BLAST search in *P. uenonis* CCUG 48615 (Supplemental Table 6).
289
290 *Phylogenetic Analysis.* 16S rRNA gene sequences were collected using the Integrated Microbial
291 Genomes & Microbiomes (IMG/MER) (70) or National Center for Biotechnology Information (NCBI)

databases for each *Porphyromonas* species reported in the human urogenital tract by Acuna-Amador in their comprehensive review (14). Uncultured and recently cultured *Porphyromonas* species were also included (71, 72). Nomenclature choices were informed by the ANI tool within IMG/MER and the Genome Taxonomy Database (GTDB, Release 06-RS202, April 27th, 2021) (73). Whenever possible, type strain and near full-length sequences were selected. Multiple sequence alignment was performed with SINA aligner (v.1.2.11) (74) using Silva's Alignment, Classification and Tree Service (ACT) (75). The phylogenetic tree was computed using RAxML v.8.2.9 (76) with the Gamma model for likelihoods (also through ACT). The tree was edited using the interactive Tree of Life (iTOL (77)). The AA identity of PepO orthologues in each *Porphyromonas* species was queried through BLASTP searches in IMG/MER and NCBI using the *P. asaccharolytica* AA sequence as the query. With the exception of *P. uenonis* 60.3, the AA identity reported corresponds with a hit showing >98% query coverage.

Construct cloning and *in vitro* transcription/translation

The Poras_0079 (PepO; IMG Gene ID 2504823953) DNA fragment encoding amino acid residues C21 to W682 was PCR amplified from a *P. asaccharolytica* DSM 20707 genomic DNA extraction (Qiagen DNeasy Blood & Tissue Kit, Germantown, MD) using the forward (5'-ATATCCATGGCTTGTAACAAGAAGCAGGAGAATC-3') and reverse primers (5'-ATATCCCGGGCCAGACCACGACACGCTC-3'). The amplicon was cloned into the pTXTL-T7p14-aH plasmid (replacing alpha hemolysin, Daicel Arbor Biosciences, Ann-Arbor, MI) using NcoI-HF and SmaI (New England Biolabs, Ipswitch, MA). The new plasmid construct (pSLP15) was transformed into *Escherichia coli* DH5α chemically competent cells and prepped using the QIAprep spin miniprep kit (Qiagen). Plasmid concentrations were determined using the Qubit dsDNA broad range assay kit with a Qubit 3 fluorometer (Invitrogen). *In vitro* myTXTL reactions were prepared by combining 5 nM of pSLP15, 1 nM of pTXTL-P70a-T7rnap (expressing the T7 RNA polymerase, Daicel Arbor BioSciences, Ann-Arbor, MI) and 9 µl of myTXTL Sigma 70 Master Mix (Arbor Biosciences) to a final volume of 12 µL with HyClone HyPure water H_2O (Cytiva); negative controls included 1 nM pTXTL-P70a-T7rnap and myTXTL Sigma 70 Master Mix only. For each reaction, 10 µL was transferred to a PCR-clean

polypropylene V bottom 96-well plate and covered with a silicone seal (Eppendorf, Mississauga, ON). Reactions were incubated at 29°C for 16 hours and final reactions stored at -20°C. To assess proteolytic activity, control (RNAP only) and PepO reactions were incorporated into fluorescent caseinase assays and collagenase assays. For caseinase assays, TXTL reactions were diluted 60-fold in TBS and 10 µL was added to each well. For type I and type IV collagenase assays, 10 µL of undiluted TXTL reactions were added to each well. Caseinase and type I collagenase assays were also conducted in the presence of 0.5 mM 1,10-phenanthroline. Mean fluorescence readings of the negative control (substrate with RNAP TXTL reaction) were subtracted from the experimental wells and relative fluorescence units (RFU) was plotted over time, with negative values adjusted to zero.

Statistical Analyses. Statistics were performed in GraphPad Prism or Stata and graphs were prepared in GraphPad. GraphPad was used to assess data variance and normality (Shapiro-Wilk test) and statistical significance was evaluated as described in figure legends. All schematic illustrations were created with BioRender.com.

Results

Vaginal *Porphyromonas* species degrade type I collagen, type IV collagen and casein using secreted proteases

Given their phylogenetic relatedness to the periodontal pathogen, *P. gingivalis,* we sought to understand whether the two *Porphyromonas* species most frequently detected in the human vagina, *P. asaccharolytica* and *P. uenonis*, possess gingipain-like protease activities (14). Collagenase activity was evaluated using fluorescently quenched substrates (type I collagen or type IV collagen), where proteolytic digestion results in dequenching and measurable increases in fluorescence over time. Fluorometric collagenase assays confirmed that *P. asaccharolytica* and *P. uenonis* cell suspensions degrade type I collagen in a dose-dependent manner (Figure 1A). Next, collagenase activity was measured in cell-free supernatants from *P. asaccharolytica* and *P. uenonis.* These experiments validated that both organisms secrete proteases capable of degrading type I and type IV collagen (Figure 1B–C). Collagenase activity was further confirmed with gelatin zymography (Supplemental Figure 2), where *P. asaccharolytica* supernatants produced three distinct high molecular weight zones of clearing (~85 kdA, 95 kDa, 120 kDa), while *P. uenonis* supernatants generated four separate zones of clearing in the gel: three high molecular weight (~75 kDa, 90 kDa, 110 kDa) and one low molecular weight (30 kDa). Next, casein degradation was monitored to evaluate general proteolytic activity of *P. asaccharolytica* and *P. uenonis* secreted proteases. Due to its low-complexity tertiary structure, casein is regarded as a universal protease substrate that is highly susceptible to proteolytic degradation. Fluorometric assays revealed that supernatants from *P. asaccharolytica* and *P. uenonis* possess caseinase activity (Figure 2D). This was further confirmed using agar-based casein degradation assays, where *P. asaccharolytica, P. uenonis* and *P. gingivalis* cell suspensions all produced zones of clearing (Supplemental Figure 3). Although *P. asaccharolytica* and *P. uenonis* can degrade similar substrates to *P. gingivalis* (41), *P. gingivalis* showed substantially higher maximum fluorescence and area under the curve for collagen degradation from cell suspensions and secreted proteases (Supplemental Figure 4, Supplemental Table 1, Supplemental Table 2). The area under the curve for casein degradation by *P. gingivalis* was also much higher than for *P. asaccharolytica* or *P. uenonis,*

while the maximum fluorescence and time to maximum fluorescence for casein degradation were comparable between all three *Porphyromonas* species (Supplemental Figure 4C, Supplemental Table 2). To understand if proteolytic activity might contribute to pathogenesis in the female genital tract, we evaluated whether a common commensal vaginal microbe is also capable of degrading collagen and casein. No collagenase or caseinase activity was detected from *Lactobacillus crispatus* cell suspensions in the fluorometric collagenase or caseinase assays (Supplemental Figure 5), suggesting that proteolytic activity could be a pathogenesis mechanism for opportunistic pathogens in the vaginal niche.

P. asaccharolytica and _P. uenonis_ inhibit fibrin clot formation through fibrinogen degradation

Since gingipains are known to degrade fibrinogen and exacerbate gum bleeding (41), we next investigated whether *P. asaccharolytica* and *P. uenonis* proteases can degrade fibrinogen and impair fibrin clot formation. To evaluate direct fibrinogen degradation, cell-free media controls and cell suspensions of *P. asaccharolytica* or *P. uenonis* were incubated in the presence and absence of human fibrinogen over a 24-hour time course. Samples removed at defined intervals were separated by SDS-PAGE and stained with Coomassie Brilliant Blue. In cell-free media controls, the fibrinogen α, β and γ chains remained intact throughout the experiment and, as expected, fibrinogen chains were absent from '*P. asaccharolytica* no Fg' and '*P. uenonis* no Fg' controls (Figure 2A–B). When *P. asaccharolytica* or *P. uenonis* were incubated with fibrinogen, complete degradation of the fibrinogen α and β chains was observed after 18 hours, while the γ chain remained intact (Figure 2A–B). To determine whether fibrinogen degradation translates to impaired fibrin clotting, thrombin-induced fibrin clot formation was measured after *Porphyromonas* cell suspensions were pre-incubated with citrated plasma. A significant delay in clot formation was observed with the highest dose of *P. asaccharolytica* or *P. uenonis* (9.0×10^9 cfu/reaction) compared to the no cell control (Figure 2C, **** $p<0.0001$) or a lower dose of *P. asaccharolytica* or *P. uenonis* (Figure 2C; **** $p<0.0001$ vs. 1.5×10^8). Turbidimetry at the experimental endpoint (30 minutes) allowed for quantitative evaluation of final clot size. In keeping with clotting times from Figure 2C, fibrin clot size was significantly reduced in samples exposed to *P.*

399 *asaccharolytica* or *P. uenonis* at 9.0x10^9 cfu/reaction compared with the no cell control (Figure 2D ****
400 p<0.0001). For *P. asaccharolytica,* a significant reduction in clot size was observed in samples treated
401 with 9.0x10^9 cfu/reaction when compared to 1.5x10^8 cfu/reaction (Figure 2D, *** p<0.0003). Similarily,
402 clot sizes in samples treated with the highest dose of *P. uenonis* (9.0x10^9 cfu/reaction) were
403 significantly smaller than samples treated with a lower doses of *P. uenonis* (Figure 2D vs. 1.5x10^8
404 cfu/reaction ** p=0.003). These findings were further confirmed by visual assessment of clot formation
405 at assay endpoints (Figure 2E). Taken together, these results show that *P. asaccharolytica* and *P.*
406 *uenonis* impair clot formation through proteolytic degradation of fibrinogen.
407
408 **Vaginal *Porphyromonas* species do not encode gingipain orthologs**
409 Given the gingipain-like proteolytic activity observed in *P. asaccharolytica* and *P. uenonis*
410 (Figures 1–2), we sought to confirm an earlier report that these organisms do not encode gingipain
411 orthologs (78). Using BLASTP, gingipain protein sequences (RgpA, RgpB, Kgp) were queried against
412 *P. asaccharolytica* and *P. uenonis* genomes (Supplemental Figure 6A), yielding zero hits in *P.*
413 *asaccharolytica* and two hits in each *P. uenonis* 23387 genome (IMG Genome ID 2585427891 and
414 2528311143); of note, these *P. uenonis* genomes were not queried in the previous analysis (78). No
415 BLASTP hits were identified in *P. uenonis* 60-3 as previously reported (78). One hit resulted from the
416 Kgp BLAST search only (Supplemental Table 3; L215DRAFT_00230/JCM13868DRAFT_00677; 27%
417 sequence identity) and another hit resulting from both the Kgp and RgpA BLAST queries (Supplemental
418 Table 3; L215DRAFT_00128/JCM13868DRAFT_01423; 26–27% sequence identity). We further
419 considered whether secreted proteases in *P. asaccharolytica* and *P. uenonis* share protein domains
420 with gingipains. Evaluation of protein families (Pfams) in the gingipains revealed four conserved protein
421 family (Pfam) domains, with RgpB containing one additional Pfam not found in RgpA or Kgp
422 (Supplemental Table 4). All five Pfams were searched against all available genomes of *P.*
423 *asaccharolytica* and *P. uenonis* to identify proteins containing gingipain Pfams (Supplemental Figure
424 6A). The peptidase C25 family (PF01364) search resulted in one hit in each of the genomes queried,
425 while the cleaved adhesin domain (PF07675) returned hits in all *P. uenonis* strains, but none in *P.*

426 *asaccharolytica* (Supplemental Table 4). To determine whether any hits from the BLAST search
427 (Supplemental Table 3) and Pfam search (Supplemental Table 4) are gingipain orthologs, we
428 performed a reciprocal BLASTP search against *P. gingivalis* (Supplemental Figure 6A). The C25
429 peptidase-containing proteins identified in the Pfam search against *P. asaccharolytica* (Poras_0230)
430 and *P. uenonis* (L215DRAFT_00971) displayed the highest percent identity with the gingipains. When
431 these sequences were queried against *P. gingivalis* using BLASTP, PGN_0022 emerged as the only
432 significant hit with 36-37% identity and 97% query coverage (Supplemental Table 5). Since PGN_0022
433 has been characterized as PorU, the type 9 secretion sortase enzyme in *P. gingivalis* (79), the C25
434 peptidase-containing proteins identified in *P. asaccharolytica* and *P. uenonis* are likely to function as
435 PorU orthologs rather than gingipains. Querying the cleaved adhesin domain-containing proteins from
436 *P. uenonis* against *P. gingivalis* revealed two uncharacterized proteins: PGN_1611 and PGN_1733 as
437 the top BLASTP hits (Supplemental Table 5). The Lys-gingipain (Kgp) was identified as fourth hit from
438 both *P. uenonis* cleaved adhesin domain-containing protein BLASTP searches (Supplemental Table 5),
439 but the percent identity and coverage are restricted to the shared pfam. Furthermore, results from
440 multiple sequence alignments with the *P. gingivalis* gingipains showed ≤20% identity for all *P.*
441 *asaccharolytica* and *P. uenonis* sequences. In summary, since all BLASTP alignments were less than
442 200 residues, full length alignments of query and subject sequences were ≤20%, reciprocal BLASTP
443 searches did not return *P. gingivalis* gingipains as top hits, and our Pfam search did not identify *P.*
444 *asaccharolytica* or *P. uenonis* proteins that appear to be gingipains, we concluded that these vaginal
445 *Porphyromonas* species do not encode gingipain orthologs.
446
447 **Identification of collagenase candidates in *P. asaccharolytica* and *P. uenonis***
448 To identify other candidate proteins that may be responsible for the collagenolytic activity of
449 vaginal *Porphyromonas* species, we first queried the MEROPs database (65) uncovering 59 and 63
450 known and predicted peptidases from *P. asaccharolytica* and *P. uenonis,* respectively. To identify
451 putative collagenase enzymes from this list, we cross-referenced these peptidases with a list of protein
452 annotation identifiers from known and predicted microbial collagenases in the BRENDA enzyme

453 information database (66). This approach shortened the candidate peptidase list to 18 enzymes in *P.*
454 *asaccharolytica* and 14 in *P. uenonis*. InterPro scans of each putative collagenase revealed proteins
455 likely to be involved in cell wall synthesis or export machinery and narrowed the list to ten peptidases in
456 *P. asaccharolytica* and nine peptidases in *P. uenonis* (Supplemental Figure 6B). Factoring in similarity
457 to characterized collagenases, additional domains identified in InterPro and the presence of secretion
458 signals, a final short list of the seven most promising candidate peptidases in each organism was
459 generated (Table 1). Intriguingly, each organisms' candidate collagenases could be organized into four
460 groups: Ig-containing serine proteases (2x), C10 cysteine proteases (2x), M13 metalloproteases (1x)
461 and U32 proteases (2x) (Table 1). Multiple sequence alignments of candidate collagenase pairs for a
462 given type within each strain revealed low sequence identity (29%–45% (Table 1)). Conversely, BLAST
463 searches between species allowed for identification of orthologous protein pairs in *P. asaccharolytica*
464 and *P. uenonis*, with sequence identity ranging from 67% up to 100% (Table 1). Taken together, this
465 suggests that within-genome pairs of candidate collagenases are likely to have resulted from a gene
466 duplication event prior to speciation of *P. asaccharolytica* and *P. uenonis.*
467 Serine proteases within the short list all contained Ig-like folds (Table 1), which are also present
468 in the binding domain of the well-characterized collagen degrading metalloproteases from *Clostridium*
469 *histolyticum* (ColG, ColH) (80). The candidate cysteine proteases contained type 9 secretion system
470 signal domains and a SpeB domain (Table 1), indicating sequence similarity with *Streptococcus*
471 *pyogenes* streptopain, a cysteine protease capable of cleaving host components such as fibrinogen,
472 immunoglobulins and complement proteins (81-83). The candidate metalloproteases from *P.*
473 *asaccharolytica* (Poras_0079) and *P. uenonis* (Poru_00076) each contained a catalytic collagenase
474 domain in addition to an M13 type metallopeptidase domain and a predicted N-terminal secretion signal
475 (Table 1). Finally, two U32 collagenases were detected in each vaginal *Porphyromonas* species
476 indicating an orthologous relationship with the *P. gingivalis* U32 collagenase PrtC (84, 85). Of note,
477 none of these putative U32 collagenases were found to possess secretion signals indicative of
478 localization to the extracellular space (Table 1).
479

480 **Vaginal *Porphyromonas* species encode metalloproteases targeting collagens, casein and**
481 **fibrinogen**

482 To narrow down candidate enzymes responsible for collagenolytic and fibrinogenolytic activities,
483 inhibitors of the predicted serine, cysteine and metalloproteases (Table 1) were incorporated into
484 functional assays. Cell-free supernatants from *P. asaccharolytica* and *P. uenonis* were incubated with
485 type I collagen in the presence of three doses of 1,10-phenanthroline, iodoacetamide or aprotinin to
486 inhibit metallo-, cysteine and serine proteases, respectively (Figure 3A–D, Supplemental Figure 6A–F).
487 Treatment of *P. asaccharolytica* supernatants with 1,10-phenanthroline resulted in decreased
488 collagenase activity, with a statistically significant reduction in max enzyme activity observed with the
489 highest dose of inhibitor (Figure 3A–B; * 0.2 mM vs. 0.02 mM p=0.004; ** 0.2 mM vs. 0.002 mM
490 p<0.0001, Supplemental Figure 6A). Iodoacetamide treatment revealed a trend toward a dose-
491 dependent decrease in collagenase activity in individual experiments (Supplemental Figure 7), but this
492 trend was not observed when multiple experiments were combined (Figure 3A–B, Supplemental Figure
493 6). However, when *P. asaccharolytica* supernatants were treated with a combination of 1,10-
494 phenanthroline and iodoacetamide, there was a further reduction in collagenase activity compared to
495 the 1,10-phenanthroline only treatment (Figure 3A–B, 1,10-Ph 0.2 mM vs. 1,10-Ph + Iodo * p=0.0378,
496 Supplemental Figure 6). Although aprotinin treatment revealed a trend towards decreased activity in the
497 time-course, there was no statistically significant decrease in max collagenase activity (Figure 3A–B,
498 Supplemental Figure 6). For *P. uenonis,* 1,10-phenanthroline also inhibited collagenase activity (Figure
499 3C–D, Supplemental Figure 6), with a significant reduction in max collagenase activity (Figure 3D; 0.2
500 mM vs. 0.02 mM p=0.002; 0.2 mM vs. 0.002 mM p=0.0043). However, treatment with aprotinin or
501 iodoacetamide did not reduce *P. uenonis* collagenase activity (Figure 3C–D, Supplemental Figure 6)
502 and the combination treatment of 1,10-phenanthroline and iodoacetamide did not provide an additional
503 reduction in collagenase activity or max fluorescence (Figure 3C–D) as observed in *P. asaccharolytica*
504 (Figure 3A-B). Taken together, these results demonstrate that both *P. asaccharolytica* and *P. uenonis*

possess secreted metalloproteases that coordinate type I collagen degradation, while *P. asaccharolytica* also appears to secrete a cysteine protease capable of degrading type I collagen.

Next, we evaluated whether the same protease classes degrade type IV collagen and casein. For both *Porphyromonas* species, the metalloprotease inhibitor 1,10-phenanthroline completely abrogated type IV collagenase activity from supernatants, while serine and cysteine protease inhibitors did not significantly reduce activity (Figure 3E–H). *P. asaccharolytica* caseinase activity was similar to its type I collagenase activity (Figure 4A–B) as proteolytic activity was reduced by treatment with 1,10-phenanthroline, and treatment with both 1,10-phenanthroline and iodoacetamide produced an additional downward shift in enzyme activity that resulted in a significant reduction in max fluorescence when compared to the no inhibitor control (Figure 4A, C; $p=0.0413$). In keeping with the type I collagen and type IV collagen degradation results, *P. uenonis* caseinase activity was significantly decreased by treatment with the metalloprotease inhibitor 1,10-phenanthroline (Figure 4B,D no inhibitor vs. 1,10-phenanthroline $p=0.018$), while aprotinin and iodoacetamide treatment did not inhibit activity (Figure 4B,D). Further to this, the 1,10-phenanthroline/iodoacetamide combination did not offer any additional reduction in protease activity (Figure 4B,D).

Inhibitors were also incorporated into fibrinogen degradation assay to determine whether fibrinogen is proteolyzed by the same enzyme classes as those observed in our collagen and casein experiments. When *P. asaccharolytica* supernatants were incubated with fibrinogen, complete degradation of the fibrinogen α and β chains was observed after 48 hours (Figure 5A, no inhibitor), while the γ chain remained intact, producing the same degradation profile observed in experiments with cell suspensions (Figure 2A). Delayed fibrinogen degradation by *P. asaccharolytica* was observed in the presence of 1,10-phenanthroline, but not with aprotinin or iodoacetamide. This suggests that secreted metalloproteases from *P. asaccharolytica* contribute to fibrinogen degradation (Figure 5A). Fibrinogen degradation patterns from *P. uenonis* supernatants differed from the results obtained with cell suspensions. While the fibrinogen α chain was degraded after two hours, the β and γ chains remained intact for the 48-hour time-course (Figure 5B). This finding suggests that *P. uenonis* may degrade fibrinogen using both secreted and cell surface-associated proteases. Interestingly, the

secreted *P. uenonis* protease that contributes to degradation of the fibrinogen α chain is not impacted by the inhibitors included in this study (Figure 5B), implying that the secreted fibrinogenolytic enzyme from *P. uenonis* is distinct from the secreted collagen and casein degrading enzymes.

Finally, we sought to further characterize the *Porphyromonas* M13 metalloproteases identified in our bioinformatics inquiries (Table 1; Figure 6A). Exploration of other *Porphyromonas* species detected in the urogenital tract and commonly isolated from other human body sites as well, revealed that the M13 metalloproteases are ubiquitous (Figure 6B). Notably, the M13 metalloprotease in *P. gingivalis* has been previously characterized as PepO, a secreted endopeptidase involved in host attachment/invasion and proteolytic activation of endothelin, a potent peptide that induces vasoconstriction (62, 63, 86). To determine whether the vaginal *Porphyromonas* M13 metalloproteases can coordinate collagenase and caseinase activity, Poras_0079 (*pepO)*, was cloned and expressed in myTXTL *in vitro* transcription/translation system. Expression of PepO was confirmed via SDS-PAGE with the appearance of a 76 kDa protein in PepO reactions, that was absent in the control RNA polymerase only reactions (Figure 7A). Fluorescent protease assays revealed that PepO is capable of degrading casein and type I collagen, but not type IV collagen (Figure 7B–D). Further, the metalloprotease inhibitor, 1,10-phenanthroline, fully abrogated type I collagenase and caseinase activity of PepO (Figure 7B–C).

Discussion

It is well established that mucinase activity is elevated during BV (87-90), and these activities have been attributed to *Gardnerella* (89, 91) and *Prevotella* species (89, 92, 93). In support of this, sialidase activity has been utilized as a diagnostic marker for BV (92, 94-97). Although most studies have focused on degradation of mucin glycans, proteolytic activity in vaginal fluid has also been linked with BV status (56-58) and described among predominant BV-associated bacteria (59, 60). Isolates of *Prevotella bivia* from women with preterm premature rupture of membranes (PPROM) were shown to secrete proteases that degrade elastin, collagen, casein and gelatin (59). In another study screening bacterial strains from women with PPROM, preterm labour or puerperal infection, protease activity was confirmed in phylogenetically diverse Gram-negative and Gram-positive organisms. This included the BV-associated bacteria *Gardnerella vaginalis*, *Prevotella bivia* (formerly *Bacteroides bivius)* and *P. asaccharolytica* (formerly *Bacteroides asaccharolyticus*) (60). The authors found that *P. bivia* and *P. asaccharolytica* exhibited collagen and casein degradation, while *G. vaginalis* exclusively degraded casein. Our findings confirm the casein/collagen degradation capacity of *P. asaccharolytica* and extend these functional activities to *P. uenonis.* Furthermore, we demonstrate that both vaginal *Porphyromonas* species also degrade type IV collagen, commonly found in reproductive tissues (98, 99), and provide the first description of the diverse protease types capable of coordinating these activities. To understand whether proteolytic activity is also observed among commensal bacteria that inhabit the vaginal niche, we investigated proteolytic activity of *Lactobacillus crispatus*, demonstrating that *L. crispatus* is not capable of degrading type I collagen or casein. The absence of detectable proteolytic activity from a commensal *Lactobacillus* strain and the growing evidence for secreted proteolytic activity from BV-associated bacteria (59, 60), including vaginal *Porphyromonas* species, suggests that degradation of host proteins could be an important virulence trait of opportunistic pathogens in the female genital tract.

Our results demonstrate that vaginal *Porphyromonas* species are capable of directly degrading fibrinogen and impairing fibrin clot formation. Fibrinogen is detected in vaginal lavage fluid (100, 101) and is targeted by other reproductive pathogens (102, 103). Although the implications of altered fibrinogen

585 levels in the female reproductive tract are not clear, impaired clotting functions could have severe
586 consequences during labour and postpartum. Fibrinogen is known to increase substantially during
587 pregnancy (104, 105), and decreased plasma fibrinogen levels have been associated with increased
588 severity of postpartum haemorrhage (106). Further to this, genetic fibrinogen abnormalities are
589 significantly associated with miscarriage, placental abruption and postpartum hemorrhage (107-110).

590 Within the female genital tract, collagens are found within the vagina, cervix, uterus and pelvic
591 floor and their composition and content is significantly altered throughout pregnancy and during labour
592 (111). Vaginal and cervical tissue is primarily composed of fibrillar type I and III collagens, with type I
593 collagen playing a critical role in tissue integrity (112-114). Type IV collagen is typically found within
594 basement membranes and is enriched within the placenta (98). Both type I and type IV collagens are
595 found within chorioamniotic membranes at the maternal-fetal interface (99). During pregnancy, cervical
596 collagens (type I, III) undergo a shift toward increased solubility and decreased abundance, contributing
597 to cervical softening (115-117), while increased collagenase activity is observed during cervical ripening
598 to prepare for dilation and parturition (118, 119). Importantly, cervical remodelling during term and
599 preterm labour occurs via the same mechanisms with host matrix metalloproteinases (MMPs)
600 coordinating cervical collagen degradation (120). Premature preterm rupture of the membrane
601 (PPROM) has been associated with infection (121, 122), increased host MMP collagenase activity
602 (123, 124) and decreased collagen content (125). Furthermore, microbial collagenases can reduce the
603 tensile strength of chorioamniotic membranes *ex vivo* (126), and collagenase activity has been
604 detected in clinical isolates from PPROM patients (59, 60). Taken together, these findings imply that
605 host and microbial modulation of collagen within the cervix and chorioamniotic membranes could play
606 critical roles in preterm labour and PPROM. In the present study, our findings indicate that *P.*
607 *asaccharolytica* and *P. uenonis* secreted proteases are capable of degrading both type I and type IV
608 collagens, uncovering a possible mechanism for how these microbes contribute to the initiation of
609 preterm labour.

610 *P. asaccharolytica* and *P. uenonis* are phylogenetically related to *P. gingivalis,* an opportunistic
611 pathogen that drives periodontal disease (30), disseminates through the bloodstream (35) and

612 contributes to adverse pregnancy outcomes (34, 127). Many of these outcomes are driven by the *P.*
613 *gingivalis* gingipains, cysteine proteases that degrade host extracellular matrix components and
614 immune factors (41). Our investigations demonstrate that *P. asaccharolytica* and *P. uenonis* possess
615 gingipain-like activities, including degradation of type I and type IV collagen, casein and fibrinogen.
616 However, key differences in total enzyme activity were observed. *P. gingivalis* supernatants possessed
617 higher total collagenase and caseinase enzyme activity than the vaginal *Porphyromonas* species based
618 on the maximum RFU, time to max RFU and area under the curve values. Previous comparative
619 genomic analyses of *Porphyromonas* species included two *P. asaccharolytica* genomes (DSM 20707,
620 PR426713P-I) and one *P. uenonis* genome (60-3), and used a reciprocal BLAST (BLASTall) to confirm
621 that *P. asaccharolytica* and *P. uenonis* do not encode gingipain orthologs (78). Expanding on these
622 findings, our study used both BLAST and domain (Pfam) queries, and included all available *P.*
623 *asaccharolytica* and *P. uenonis* genomes including two additional *P. uenonis* genomes (DSM 23387;
624 IMG Genome IDs 2528311143 and 2585427891) that were not included in the previous study. In
625 agreement with the previous study (78), our findings did not return any gingipain ortholog hits from
626 reciprocal BLASTP or Pfam searches. This absence of gingipain orthologs is in keeping with the
627 observed differences in functional proteolytic activity. Taken together, these results prompted an
628 investigation of novel candidate proteases.

629 Our bioinformatics inquiries identified five candidate secreted collagenases in each vaginal
630 *Porphyromonas* species. By incorporating protease inhibitors into our functional assays, we determined
631 that *Porphyromonas* secreted metalloproteases degrade collagens (type I, IV), casein and fibrinogen.
632 For *P. uenonis,* we observed consistent results with metalloprotease inhibitor 1,10-phenanthroline
633 exclusively inhibiting degradation with casein and collagens (type I,IV), while no inhibitors blocked
634 fibrinogen degradation. Importantly, no additional reduction in activity was observed when the cysteine
635 protease inhibitor iodoacetamide was included with 1,10-phenanthroline in type I collagenase or
636 caseinase assays, suggesting that secreted metalloproteases are solely responsible for degradation of
637 these substrates by *P. uenonis*. With *P. asaccharolytica*, on the other hand, we observed that
638 iodoacetamide caused a dose-dependent reduction in *P. asaccharolytica* type I collagenase activity.

639 Furthermore, when 1,10-phenanthroline and iodoacetamide were combined, there was an additional
640 decrease in *P. asaccharolytica* type I collagenase and caseinase activity relative to treatment with 1,10-
641 phenanthroline alone. These results suggest that although *P. asaccharolytica* and *P. uenonis* possess
642 the same candidate collagenases, only *P. asaccharolytica* appears to secrete both metallo and cysteine
643 proteases in the experimental conditions used in our study. This is further supported by collagen
644 zymogram results, where banding patterns revealed different sizes of collagenases from *P.*
645 *asaccharolytica* and *P. uenonis.* Future investigations will need to address whether pH or redox state
646 may affect the activity of the cysteine proteases. Additionally, due to the general proteolytic activity of
647 the metallo and cysteine proteases, it is plausible that secreted proteases may degrade other proteins
648 in the supernatants, including other proteases.

649 Our bioinformatics approach highlighted the U32 collagenases as likely candidates to confer
650 proteolytic activity, however, we were unable to find any sequence-based evidence for secretion to the
651 extracellular space or localization to the cell surface in *P. asaccharolytica* or *P. uenonis*. As such, these
652 enzymes are unlikely to be found in culture supernatants. The collagenase activity of the *P. gingivalis*
653 U32 collagenase, PrtC, has been confirmed (84, 85, 128), but these studies used cell lysates (85),
654 recombinant PrtC (84) or heterologous expression systems (128). To our knowledge, no studies have
655 determined the subcellular localization of PrtC, and sequence analysis does not reveal any indication of
656 secretion signals. In fact, additional studies have confirmed that the majority of collagenase activity
657 from *P. gingivalis* is attributed to the gingipains (129, 130). On the other hand, characterized U32
658 collagenases from other bacteria are known to be secreted (131, 132). The active site residues,
659 protease type and inhibitors of U32 collagenase remain unknown, but the lack of evidence for secretion
660 in *Porphyromonas* species makes these U32 collagenases improbable candidates for the proteolytic
661 activity observed in this study.

662 Since 1,10-phenanthroline inhibited the secreted proteolytic activity of *P. asaccharolytica* and *P.*
663 *uenonis*, the M13 metalloproteases were expected to confer the observed protease activity. These
664 predicted collagenases from *P. asaccharolytica* and *P. uenonis* each contain an N-terminal signal
665 sequence, M13 peptidase domain and a catalytic collagenase domain. The *P. asaccharolytica* M13

metalloprotease was cloned and expressed in an *in vitro* transcription/translation system and confirmed to contribute type I collagenase and caseinase activity. Phylogenetic analysis of the *P. asaccharolytica* and *P. uenonis* M13 metalloproteases revealed an orthologous relationship with the *P. gingivalis* endopeptidase, PepO (PgPepO), and confirmed the presence of PepO orthologs in other vaginal and oral *Porphyromonas* species. Previous work characterizing *P. gingivalis* PepO revealed sequence conservation with the human endothelin converting enzyme 1 (ECE-1), which proteolytically processes inactive endothelin (big endothelin) into active endothelin. Activated endothelin peptides can induce vasoconstriction and cellular proliferation, alter vascular permeability and activate inflammatory cells (133, 134). PgPepO was confirmed to possess ECE-1 like activity, converting all three subtypes of big endothelin to active endothelin (62). Numerous studies have also demonstrated that PgPepO plays a role in cellular invasion and intracellular survival of *P. gingivalis* (63, 86). However additional substrates for this endopeptidase and the functional consequences of bacterial endothelin activation have yet to be explored.

PepO orthologs have also been characterized in select *Lactobacillus* species: *Lactobacillus lactis* and *Lactobacillus rhamnosus* PepO can proteolyze casein, but these enzymes are either confirmed or predicted to localize in the cytoplasm (135, 136). PepO has also been explored in *Streptococcus* species, including *Streptococcus pneumoniae* and *Streptococcus pyogenes* (Group A Streptococci; GAS). In *S. pneumoniae,* PepO is detected on the bacterial cell surface and in culture supernatants. *S. pneumoniae* PepO binds to host cells and fibronectin, facilitating bacterial adhesion and invasion (137). Streptococcal PepO also interacts with the host immune system, but there is conflicting evidence on whether this contributes to immune evasion or activation. While some studies demonstrate that *S. pneumoniae* PepO binds plasminogen and complement proteins (C1q), contributing to escape from fibrin clots and complement attack (137, 138), others demonstrate that PepO enhances macrophage autophagy and bactericidal activity via TL2/4 activation (139, 140). Surprisingly, none of these studies have shown any proteolytic activity of *S. pneumoniae* PepO. In GAS, PepO has been detected both in the cytoplasm and as a secreted protein (141, 142). Similar to *S. pneumoniae*, GAS PepO contributes to complement evasion via C1q binding (142). GAS PepO

participates in regulating quorum sensing via direct degradation of peptide pheromones secreted by GAS (141). Taken together, this body of work highlights the broad substrate specificity and diverse functionality of bacterial PepO. To our knowledge, our work characterizing *P. asaccharolytica* PepO is the first to demonstrate degradation of host extracellular matrix (type I collagen), adding another substrate to the proteolytic repertoire of PepO. The findings that PepO can degrade regulatory proteins secreted by host cells (*P. gingivalis* PepO: endothelin) and bacterial cells (GAS PepO: quorum sensing peptides) suggests that PepO enzymes could play a role in the dysregulation of proteolytic cascades. Further investigation is needed to better understand the substrates targeted by PepO proteins in complex mucosal body sites such as the female reproductive tract to reveal how this enzyme contributes to the pathogenesis of phylogenetically diverse bacteria.

Acknowledgements

The authors would like to thank Dr. Antoine Dufour and Dr. Morley Hollenberg for technical assistance and advice on this work.

Conflict of Interest

The authors declare that the research was conducted in the absence of any commercial or financial relationships that could be construed as a potential conflict of interest.

Funding

This work was supported by the Canadian Institutes of Health Research (L.K.S., FRN 161348), the National Institutes of Health (L.K.S., STI-CRC Developmental Research Program Award associated with U19AI113173), the Canadian Foundation for Innovation John R. Evans Leaders Fund (L.K.S, 36603), Alberta Innovates (K.V.L. and A.D.), the Government of Alberta, and the University of Calgary's Snyder Institute for Chronic and Infectious Diseases, International Microbiome Centre, O'Brien Centre for the Bachelor of Health Sciences (V.C.H.B.), and Program for Undergraduate Research Experience (E.K.).

Figures

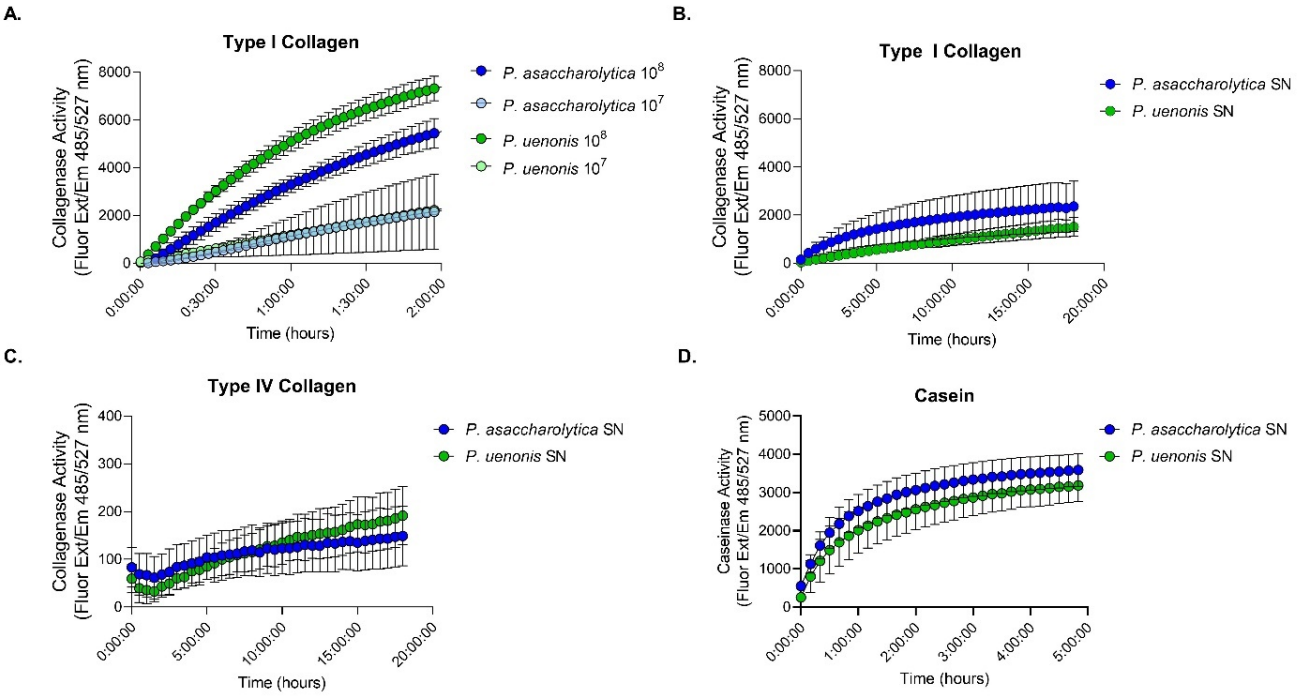

Figure 1. Proteolytic activity of vaginal *Porphyromonas* species. (A) Cell suspensions of *P. asaccharolytica* and *P. uenonis* at 10^7 or 10^8 cfu/reaction were incubated with fluorophore-conjugated type I collagen. Results are presented as mean ± standard error from three independent experiments performed in technical triplicate or quadruplicate. Collagen degradation was measured every three minutes by detecting the increase in fluorescence (Excitation 485 nm/Emission 527 nm) over a two-hour time course. **(B–C)** Cell-free supernatants of *P. asaccharolytica* and *P. uenonis* were incubated with fluorophore-conjugated **(B)** type I or **(C)** type IV collagen over an 18-hour time course; fluorescence was measured every 30 minutes. Results are presented as mean ± standard error from seven independent experiments (type I collagen) and four independent experiments (type IV collagen) performed in technical triplicate. **(D)** Cell-free supernatants of *P. asaccharolytica* and *P. uenonis* were incubated with fluorophore-conjugated casein over a five-hour time course; fluorescence was measured every ten minutes. Results are presented as mean ± standard error from five independent experiments performed in technical triplicate.

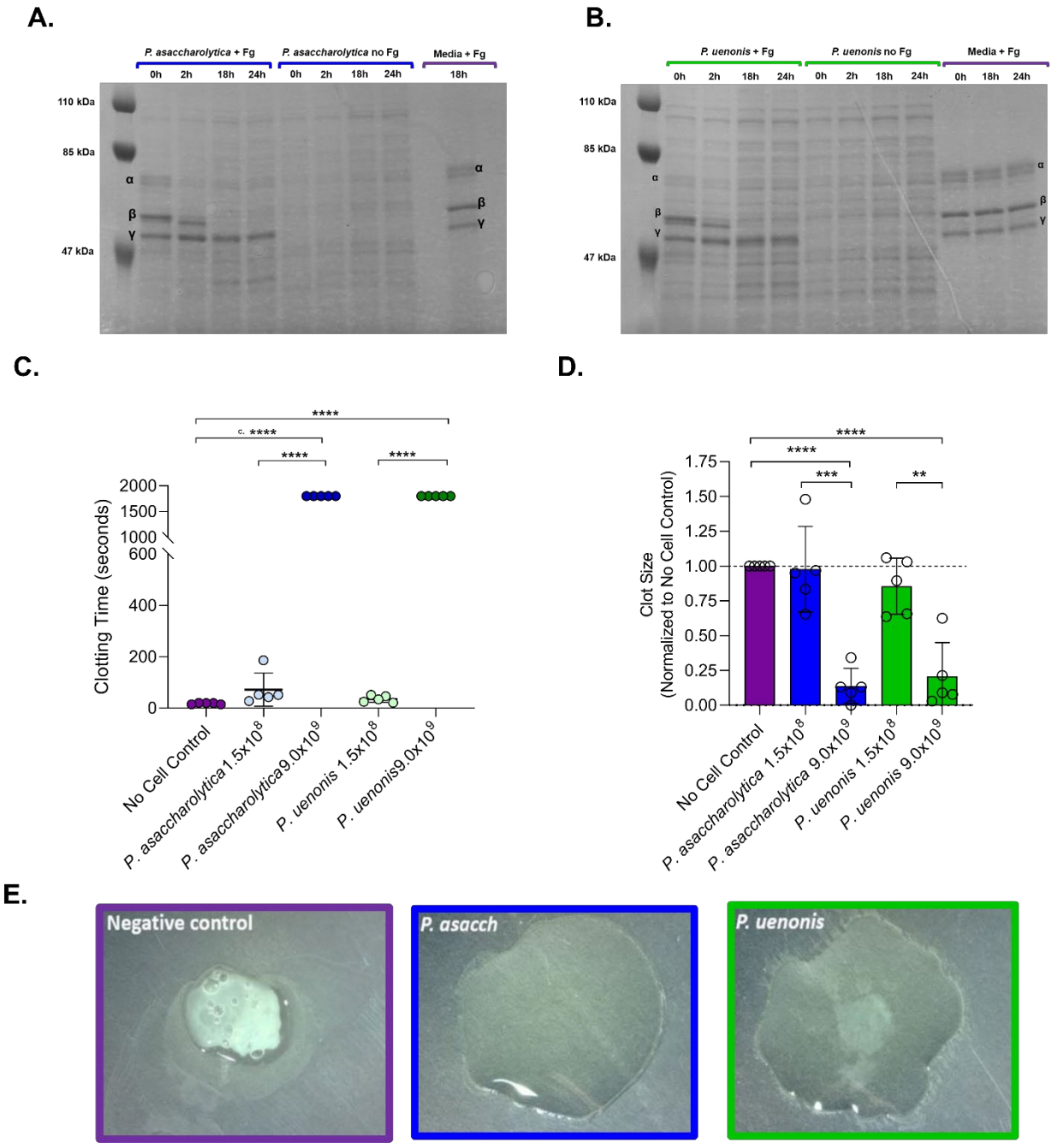

Figure 2. Vaginal *Porphyromonas* species degrade fibrinogen and impair clot formation. (A–B) SDS-PAGE of **(A)** *P. asaccharolytica* and **(B)** *P. uenonis* cell suspensions incubated with human fibrinogen (+Fg), saline (no Fg), or a cell-free media control (sBHI media +Fg). Samples collected over 24 hours were assessed for fibrinogen degradation, indicated by absence of bands corresponding to α, β, and γ fibrinogen chains in '*Porphyromonas* cells + Fg' treatments compared to 'no Fg' or media controls. **(C)** Time from thrombin addition to fibrin clot formation. Citrated plasma was pre-incubated with cell suspensions of *P. asaccharolytica* or *P. uenonis* or no cell controls. Experiments were

769 performed in technical duplicate and results are presented as mean ± standard error from five
770 independent experiments. **(D)** Quantitative evaluation of clot size at the experimental endpoint (>30
771 minutes). Following clotting time assessment, samples were subjected to well area scans at
772 absorbance 405 nm to indicate the average clot size. Experiments were performed in technical
773 duplicate and control reactions without thrombin were used to blank the experimental reactions. Data
774 were normalized to the average clot size of the no cell control within each experiment. Results are
775 presented as mean ± standard error from five independent experiments. For clotting time, significance
776 was assessed by one-way ANOVA with Holm-Sidak's multiple comparisons test where **** $p<0.0001$.
777 For endpoint clot size evaluation, significance was assessed by one-way ANOVA with Holm-Sidak's
778 multiple comparisons test where **** $p<0.0001$, *** $p<0.0003$, ** $p=0.003$ **(E)** Endpoint qualitative
779 evaluation of fibrin clots (>30 minutes) after clotting time assay with cell suspensions of *P.*
780 *asaccharolytica* ($2.4x10^9$ cfu/reaction), *P. uenonis* ($3.0x10^9$ cfu/reaction) or no cell control.
781
782
783
784
785
786
787
788
789

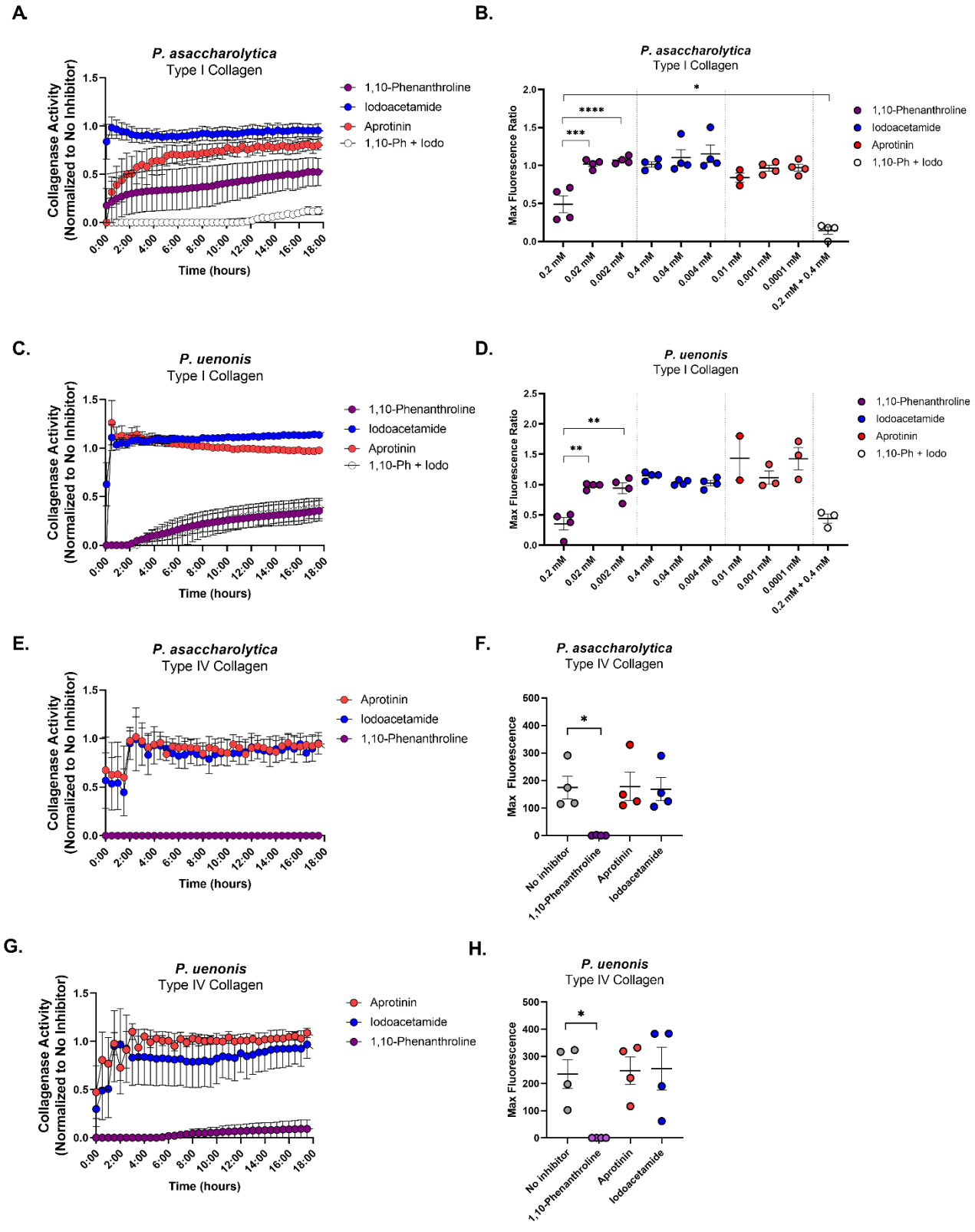

790

Figure 3. Vaginal *Porphyromonas* protease types displaying type I and type IV collagenase activity. Cell-free supernatants of **(A-B, E-F)** *P. asaccharolytica* and **(C-D, G-H)** *P. uenonis* were incubated with fluorophore-conjugated **(A-D)** type I collagen or **(E-H)** type IV collagen in the presence of the metalloprotease inhibitor 1,10-phenanthroline, the cysteine protease inhibitor, iodoacetamide, or the serine protease inhibitor, aprotinin. **(A,C)** Type I collagen degradation was measured every 30 minutes by detecting fluorescence (Excitation 485 nm/Emission 527 nm) over an 18-hour time course in the presence of 0.2 mM 1,10-phenanthroline, 0.4 mM iodoacetamide, 0.01 mM aprotinin or 0.2 mM 1,10-phenanthroline + 0.4 mM iodoacetamide. Results are presented as a ratio normalized to the no inhibitor control (set to 1.0). **(B)** Maximum fluorescence of *P. asaccharolytica* collagenase activity, expressed as a ratio normalized to the no inhibitor control, in the presence of three doses of the inhibitors. Results are presented as mean ± standard error from four independent experiments or three independent experiments (*P. asaccharolytica* + aprotinin 0.01 mM) performed in technical triplicate. Statistical significance was assessed with a one-way ANOVA and Tukey's post-hoc comparison where 1,10-phenanthroline 0.2 mM vs. 0.02 mM **** $p<0.0001$, 1,10-phenanthroline 0.2 mM vs. 0.002 mM *** $p=0.0004$ and 1,10-phenanthroline 0.2 mM vs. 0.2 mM 1,10-phenanthroline + 0.4 mM iodoacetamide * $p=0.0387$. **(D)** Maximum fluorescence ratios of *P. uenonis* collagenase activity, expressed as a ratio normalized to the no inhibitor control, in the presence of three doses of the inhibitors. Results are presented as mean ± standard error from four independent experiments or two independent experiments (*P. uenonis* + aprotinin 0.01 mM) performed in technical triplicate. Statistical significance was assessed with a one-way ANOVA and Tukey's post-hoc comparison, where 1,10-phenanthroline 0.2 mM vs. 0.02 mM ** $p=0.002$, 1,10-phenanthroline 0.2 mM vs. 0.002 mM ** $p=0.0043$. **(E-H)** Type IV collagen degradation was measured every 30 minutes by detecting fluorescence (Excitation 485 nm/Emission 527 nm) over an 18-hour time course in the presence of 0.2 mM 1,10-phenanthroline, 0.4 mM iodoacetamide, 0.01 mM aprotinin or 0.2 mM 1,10-phenanthroline + 0.4 mM iodoacetamide. Results are presented as a ratio normalized to the no inhibitor control and presented as mean ± standard error from three independent experiments performed in technical triplicate. **(F)** Maximum fluorescence of *P. asaccharolytica* supernatant collagenase activity in the presence of inhibitors.

Results are presented as mean ± standard error from four independent experiments performed in technical triplicate. Statistical significance was assessed with a one-way ANOVA and Tukey's post-hoc comparison where 1,10-phenanthroline 0.2 mM vs. no inhibitor * p=0.0352. **(H)** Maximum fluorescence of *P. uenonis* supernatant collagenase activity in the presence of inhibitors. Results are presented as mean ± standard error from four independent experiments performed in technical triplicate. Statistical significance was assessed with a one-way ANOVA and Tukey's post-hoc comparison where 1,10-phenanthroline 0.2 mM vs. no inhibitor * p=0.0398.

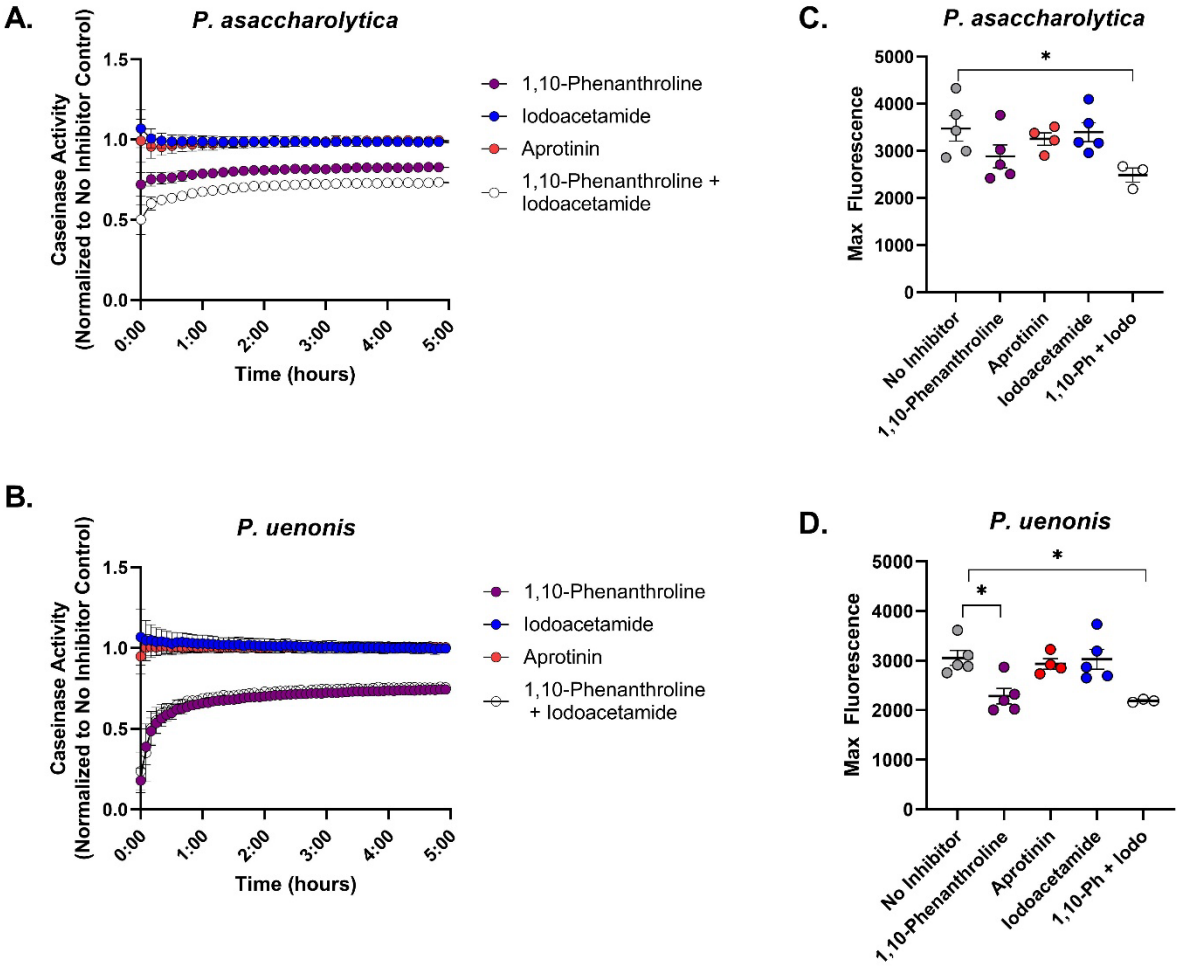

Figure 4. *P. asaccharolytica* and *P. uenonis* secreted metalloproteases have broad substrate specificity. (A-B) Cell-free supernatants of **(A)** *P. asaccharolytica* and **(B)** *P. uenonis* were incubated with fluorophore-conjugated casein in the presence of the metalloprotease inhibitor 1,10-phenanthroline (0.2 mM), the cysteine protease inhibitor iodoacetamide (0.4 mM), or the serine protease inhibitor aprotinin (0.01 mM). Casein degradation was measured every 10 minutes by detecting the increase in fluorescence (Excitation 485 nm/Emission 527 nm) over a 5-hour time course. Results are presented as a ratio normalized to the no inhibitor control and presented as mean ± standard error from five independent experiments performed in technical triplicate. **(C)** Maximum fluorescence of *P. asaccharolytica* supernatant caseinase activity in the presence of inhibitors. Results are presented as mean ± standard error from five independent experiments performed in technical triplicate. Statistical significance was assessed with a one-way ANOVA and Tukey's post-hoc comparison, where inhibitor combination vs. no inhibitor * p=0.0413. **(D)** Maximum fluorescence of *P. uenonis* supernatant

caseinase activity in the presence of inhibitors. Results are presented as mean ± standard error from five independent experiments performed in technical triplicate. Statistical significance was assessed with a one-way ANOVA and Tukey's post-hoc comparison, where 1,10-phenanthroline 0.2 mM vs. no inhibitor p=0.0145, inhibitor combination vs. no inhibitor p=0.0180.

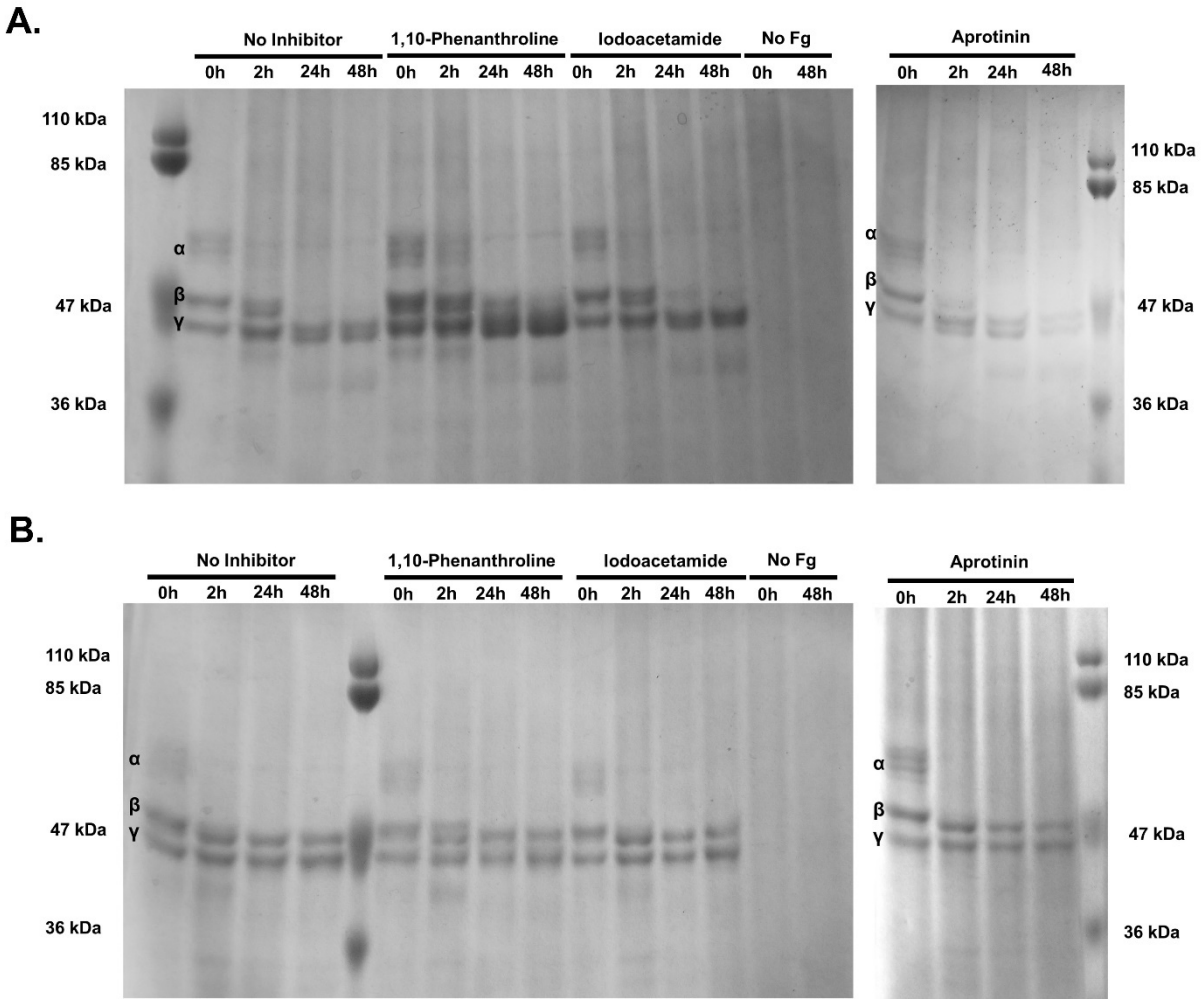

Figure 5. *P. asaccharolytica* metalloproteases degrade fibrinogen. (A) SDS-PAGE of *P. asaccharolytica* supernatants incubated with human fibrinogen in the presence of 1,10-phenanthroline (0.5 mM), iodoacetamide (1mM) or aprotinin (0.01 mM) compared to no inhibitor and no fibrinogen controls. Samples collected over 48 hours were assessed for fibrinogen degradation, indicated by absence of bands corresponding to α, β, and γ fibrinogen chains as denoted within gel images. **(B)** SDS-PAGE of *P. uenonis* supernatants incubated with human fibrinogen in the presence of 1,10-phenanthroline (0.5 mM), iodoacetamide (1mM) or aprotinin (0.01 mM) compared to no inhibitor and no fibrinogen controls. Samples collected over 48 hours were assessed for fibrinogen degradation, indicated by absence of bands corresponding to α, β, and γ fibrinogen chains.

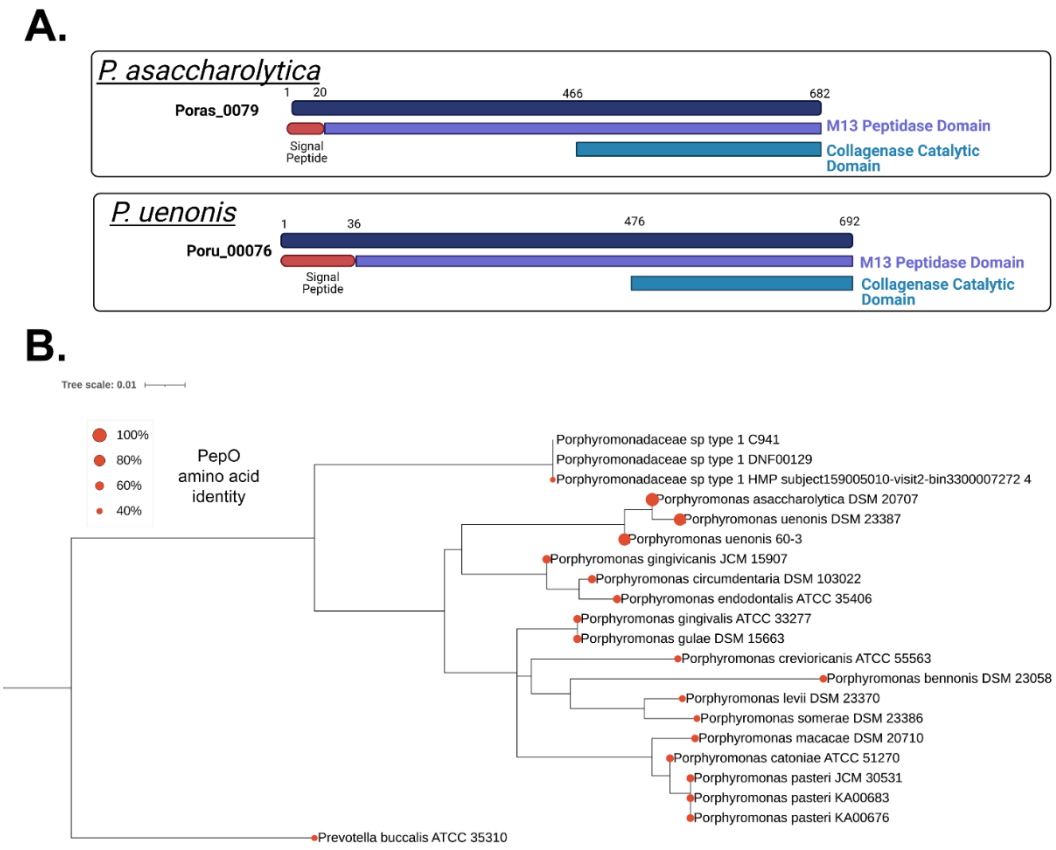

Figure 6. Secreted PepO metallopeptidases identified in *P. asaccharolytica* and *P. uenonis*. **(A)** Domain structure of candidate host-degrading PepO metalloproteases from *P. asaccharolytica* and *P. uenonis*. **(B)** 16S rRNA gene phylogeny of *Porphyromonas* species identified in the urogenital tract. The Maximum Likelihood tree was created using RAxML and rooted to *Prevotella buccalis* (same order, different family). Red circles on each leaf indicate the percent amino acid identity of that species' PepO ortholog compared to *P. asaccharolytica* PepO (Poras_0079 = 100%). The taxon previously identified as uncultivated *Porphyromonas* species type 1 was found to encompass two cultured, but unsequenced isolates (DNF00129 and C941, >99% 16S rRNA gene identity over 1120 nt). We also identified a metagenome assembled genome (MAG) in IMG/MER that encoded a 958 bp 16S rRNA gene fragment >99.5% identical to those from the cultured isolates DNF00129 and C941. Since this MAG represents the only genome sequence available for this species, we used it in our PepO queries, identifying an orthologue 42% identical to *P. asaccharolytica* PepO. Since this taxon's PepO ortholog was more distantly related to *P. asaccharolytica* PepO than the PepO ortholog identified in *Prevotella*

buccalis (47% identical), it may represent a novel genus or family; we therefore chose to label this taxon *Porphyromonadaceae* sp. type 1. Our phylogenetic analysis, along with inquiries through the Genome Taxonomy Database, furthermore indicated that vaginal isolates KA00683 and KA00676 should be designated as belonging to the species *P. pasteri*, with each containing a PepO ortholog 58–59% identical to that from *P. asaccharolytica*.

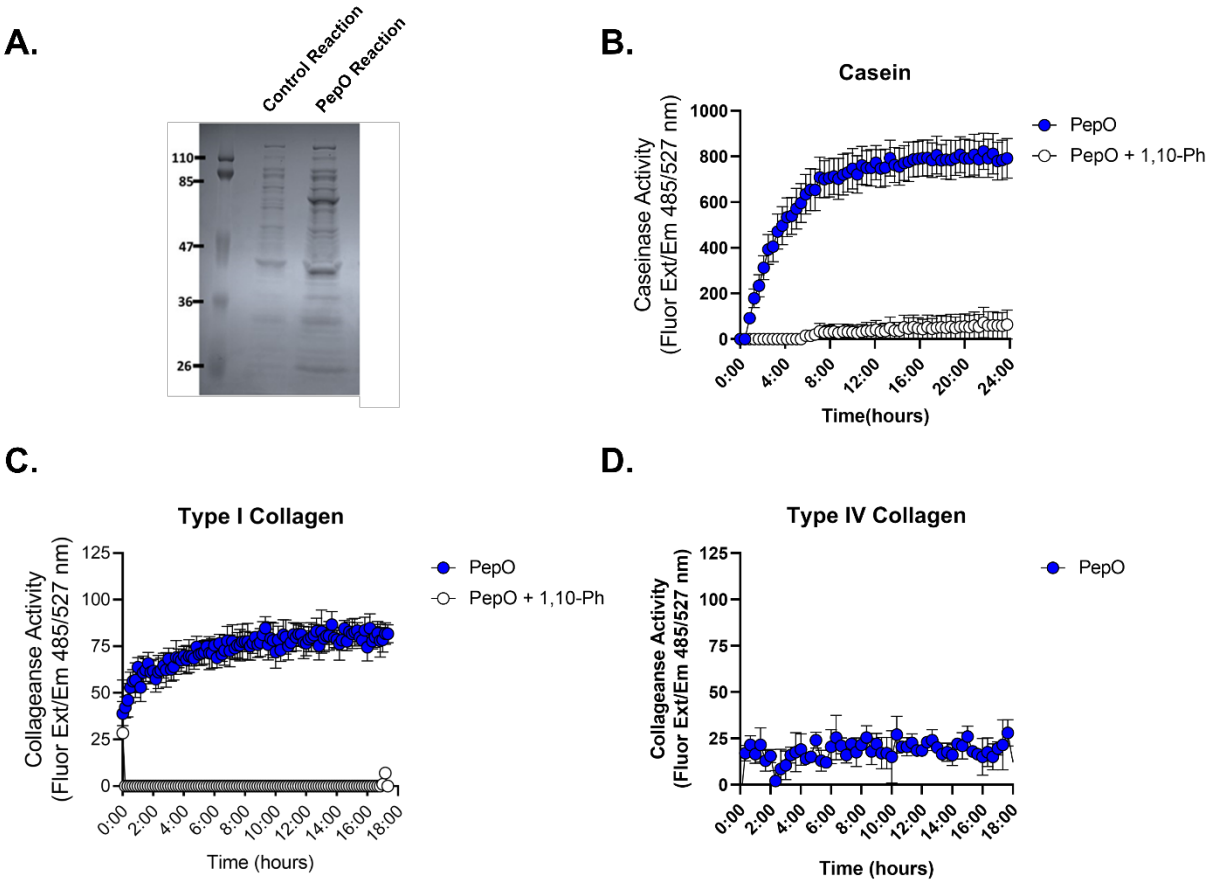

Figure 7. The *P. asaccharolytica* metalloprotease PepO degrades casein and type I collagen **(A)** SDS-PAGE of control *in vitro* transcription/translation (TXTL) reaction (RNA polymerase only) and PepO TXTL reaction. **(B-D)** PepO TXTL reactions were incubated with **(B)** FITC-casein or **(C)** fluorophore-conjugated type I collagen in the presence of 0.5 mM 1,10-phenantrholine. Casein degradation was measured every 30 minutes by detecting the increase in fluorescence (Excitation 485 nm/Emission 527 nm) over a 24-hour time course and results are presented as mean ± standard error from three independent experiments. Collagen degradation was measured every 10 minutes by detecting the increase in fluorescence (Excitation 485 nm/Emission 527 nm) over an 18-hour time course. Results are presented as mean ± standard error from five independent experiments. **(D)** PepO TXTL reactions were incubated with type IV collagen over an 18-hour time course and results are presented as mean ± standard deviation from one independent experiment.

Tables

Table 1. Candidate collagenases in *P. asaccharolytica* and *P. uenonis*.

Protease Type	*P. asaccharolytica* DSM 20707				*P. uenonis* DSM 23387				Interstrain Identity*
	Gene	Collagenase IDs[=]	Secretion	Intrastrain Identity*	Gene	Collagenase IDs[=]	Secretion	Intrastrain Identity*	
Ig-containing Serine Protease[%]	Poras_1474	IPR013783 IPR026444 TIGR04183	Type IX[#], Sec/SPII[&]	45.1%	Poru_01109	IPR013783 IPR026444 TIGR04183	Type IX[#], Sec/SPI[&]	35.2%	77.5%
	Poras_0168	IPR013783 IPR026444 TIGR04183	Type IX[#]		Poru_00939	IPR13783 IPR026444 TIGR0483	Type IX[#], Sec/SPI[&]		100%
M13 Metalloprotease[$]	Poras_0079	IPR024079	Sec/SPII[&]	N/A	Poru_00076	IPR024079	Sec/SPII[&]	N/A	92.7%
C10 Protease[@]	Poras_1659	IPR026444	Type IX[#], Sec/SPI[&]	31.3%	Poru_01083	IPR026444 TIGR0483	Type IX[#]	28.8%	67.2%
	Poras_0891	IPR026444	Type IX[#], Sec/SPI[&]		Poru_00099	IPR026444 TIGR0483	Type IX[#], Sec/SPI[&]		72.8%
U32 Collagenase[+]	Poras_0217	U32.003 PF12392 PF01136 IPR020988 IPR001539 PS01276	N/A	29.3%	Poru_01540	PF01136 PF12392	N/A	29.0%	90.6%

	Poras_0873	PF01136 U32.003 IPR001539 PS01276	N/A		Poru_00228	PF01136 PF12392	N/A		97.3%

All peptidases from *P. asaccharolytica* and *P. uenonis* were populated in UniProt using the advanced search tool to identify proteins with MEROPs annotations. Peptidases were cross-referenced against protein annotation identifiers in known and predicted microbial collagenases (BRENDA enzyme number: EC3.4.24.3) and the most promising candidate collagenases were selected by exploration of each entry in InterPro, Uniprot and MEROPS to identify important domains, secretion signals and predicted inhibitors. Any proteins involved in cell wall synthesis were eliminated.
Predicted inhibitors (MEROPS): [%]Aprotinin, Bowman-Birk, Serpins; [$]1,10-phenanthroline, phosphoramidon, [@]Iodoacetamide, N-ethylmaleimide, [+] N/A
[=]Collagenase IDs (BRENDA enzyme #: EC3.4.24.3, InterPro, Pfam or MEROPs IDs): IPR013783: Ig-like fold; IPR026444: C-term sec signal; TIGR04183: PorC sec signal; IPR024079: metallopeptidase catalytic domain; TIGR0483: Por sec system; PF01136; PF12392; U32.003: salmonella type collagenase; PF12392: Collagenase; PF01136: Peptidase U32; IPR020988: Peptidase U32, collagenase; IPR001539: Peptidase U23, bacterial collagenases; PS01276: Peptidase family U32; PF01136 Peptidase family U32; PF12392 collagenase
[#]Type IX secretion determined by presence of IDs: TIGR0483, IPR026444, or PF18962 from TIGR Fam, InterPro and Pfam, in the protein C-terminus
[&]SignalP prediction
*Clustal Omega multiple sequence alignment
^Locus tags correspond to L215DRAFT_XXXXX

References

1. van de Wijgert JH, Borgdorff H, Verhelst R, Crucitti T, Francis S, Verstraelen H, et al. The vaginal microbiota: what have we learned after a decade of molecular characterization? PLoS One. 2014;9(8):e105998.
2. Ravel J, Gajer P, Abdo Z, Schneider GM, Koenig SS, McCulle SL, et al. Vaginal microbiome of reproductive-age women. Proc Natl Acad Sci U S A. 2011;108 Suppl 1:4680-7.
3. Onderdonk AB, Delaney ML, Fichorova RN. The Human Microbiome during Bacterial Vaginosis. Clin Microbiol Rev. 2016;29(2):223-38.
4. Cohen CR, Lingappa JR, Baeten JM, Ngayo MO, Spiegel CA, Hong T, et al. Bacterial vaginosis associated with increased risk of female-to-male HIV-1 transmission: a prospective cohort analysis among African couples. PLoS Med. 2012;9(6):e1001251.
5. Brotman RM, Klebanoff MA, Nansel TR, Yu KF, Andrews WW, Zhang J, et al. Bacterial vaginosis assessed by gram stain and diminished colonization resistance to incident gonococcal, chlamydial, and trichomonal genital infection. J Infect Dis. 2010;202(12):1907-15.
6. Myer L, Denny L, Telerant R, Souza M, Wright TC, Jr., Kuhn L. Bacterial vaginosis and susceptibility to HIV infection in South African women: a nested case-control study. J Infect Dis. 2005;192(8):1372-80.
7. Hillier SL, Nugent RP, Eschenbach DA, Krohn MA, Gibbs RS, Martin DH, et al. Association between bacterial vaginosis and preterm delivery of a low-birth-weight infant. The Vaginal Infections and Prematurity Study Group. N Engl J Med. 1995;333(26):1737-42.
8. Fettweis JM, Serrano MG, Brooks JP, Edwards DJ, Girerd PH, Parikh HI, et al. The vaginal microbiome and preterm birth. Nat Med. 2019;25(6):1012-21.
9. Elovitz MA, Gajer P, Riis V, Brown AG, Humphrys MS, Holm JB, et al. Cervicovaginal microbiota and local immune response modulate the risk of spontaneous preterm delivery. Nat Commun. 2019;10(1):1305.
10. Norenhag J, Du J, Olovsson M, Verstraelen H, Engstrand L, Brusselaers N. The vaginal microbiota, human papillomavirus and cervical dysplasia: a systematic review and network meta-analysis. BJOG. 2020;127(2):171-80.
11. Klein C, Kahesa C, Mwaiselage J, West JT, Wood C, Angeletti PC. How the Cervical Microbiota Contributes to Cervical Cancer Risk in Sub-Saharan Africa. Front Cell Infect Microbiol. 2020;10:23.
12. Laniewski P, Barnes D, Goulder A, Cui H, Roe DJ, Chase DM, et al. Linking cervicovaginal immune signatures, HPV and microbiota composition in cervical carcinogenesis in non-Hispanic and Hispanic women. Sci Rep. 2018;8(1):7593.
13. Srinivasan S, Morgan MT, Liu C, Matsen FA, Hoffman NG, Fiedler TL, et al. More than meets the eye: associations of vaginal bacteria with gram stain morphotypes using molecular phylogenetic analysis. PLoS One. 2013;8(10):e78633.
14. Acuna-Amador L, Barloy-Hubler F. Porphyromonas spp. have an extensive host range in ill and healthy individuals and an unexpected environmental distribution: A systematic review and meta-analysis. Anaerobe. 2020;66:102280.
15. McClelland RS, Lingappa JR, Srinivasan S, Kinuthia J, John-Stewart GC, Jaoko W, et al. Evaluation of the association between the concentrations of key vaginal bacteria and the increased risk of HIV acquisition in African women from five cohorts: a nested case-control study. Lancet Infect Dis. 2018;18(5):554-64.
16. Hillier SL, Krohn MA, Rabe LK, Klebanoff SJ, Eschenbach DA. The normal vaginal flora, H2O2-producing lactobacilli, and bacterial vaginosis in pregnant women. Clin Infect Dis. 1993;16 Suppl 4:S273-81.

17. Zozaya-Hinchliffe M, Lillis R, Martin DH, Ferris MJ. Quantitative PCR assessments of bacterial species in women with and without bacterial vaginosis. J Clin Microbiol. 2010;48(5):1812-9.
18. Delaney ML, Onderdonk AB. Nugent score related to vaginal culture in pregnant women. Obstet Gynecol. 2001;98(1):79-84.
19. Albert AY, Chaban B, Wagner EC, Schellenberg JJ, Links MG, van Schalkwyk J, et al. A Study of the Vaginal Microbiome in Healthy Canadian Women Utilizing cpn60-Based Molecular Profiling Reveals Distinct Gardnerella Subgroup Community State Types. PLoS One. 2015;10(8):e0135620.
20. Schellenberg JJ, Links MG, Hill JE, Dumonceaux TJ, Kimani J, Jaoko W, et al. Molecular definition of vaginal microbiota in East African commercial sex workers. Appl Environ Microbiol. 2011;77(12):4066-74.
21. Holst E, Goffeng AR, Andersch B. Bacterial vaginosis and vaginal microorganisms in idiopathic premature labor and association with pregnancy outcome. J Clin Microbiol. 1994;32(1):176-86.
22. Petrina MAB, Cosentino LA, Wiesenfeld HC, Darville T, Hillier SL. Susceptibility of endometrial isolates recovered from women with clinical pelvic inflammatory disease or histological endometritis to antimicrobial agents. Anaerobe. 2019;56:61-5.
23. Haggerty CL, Hillier SL, Bass DC, Ness RB. Bacterial vaginosis and anaerobic bacteria are associated with endometritis. Clin Infect Dis. 2004;39(7):990-5.
24. Chao X, Sun T, Wang S, Tan X, Fan Q, Shi H, et al. Research of the potential biomarkers in vaginal microbiome for persistent high-risk human papillomavirus infection. Ann Transl Med. 2020;8(4):100.
25. Chen Y, Qiu X, Wang W, Li D, Wu A, Hong Z, et al. Human papillomavirus infection and cervical intraepithelial neoplasia progression are associated with increased vaginal microbiome diversity in a Chinese cohort. BMC Infect Dis. 2020;20(1):629.
26. Walther-Antonio MR, Chen J, Multinu F, Hokenstad A, Distad TJ, Cheek EH, et al. Potential contribution of the uterine microbiome in the development of endometrial cancer. Genome Med. 2016;8(1):122.
27. Summanen PH, Durmaz B, Vaisanen ML, Liu C, Molitoris D, Eerola E, et al. Porphyromonas somerae sp. nov., a pathogen isolated from humans and distinct from porphyromonas levii. J Clin Microbiol. 2005;43(9):4455-9.
28. Eloe-Fadrosh EA, Rasko DA. The human microbiome: from symbiosis to pathogenesis. Annu Rev Med. 2013;64:145-63.
29. Yang HW, Huang YF, Chou MY. Occurrence of Porphyromonas gingivalis and Tannerella forsythensis in periodontally diseased and healthy subjects. J Periodontol. 2004;75(8):1077-83.
30. How KY, Song KP, Chan KG. Porphyromonas gingivalis: An Overview of Periodontopathic Pathogen below the Gum Line. Front Microbiol. 2016;7:53.
31. Hajishengallis G, Darveau RP, Curtis MA. The keystone-pathogen hypothesis. Nat Rev Microbiol. 2012;10(10):717-25.
32. Katz J, Yang QB, Zhang P, Potempa J, Travis J, Michalek SM, et al. Hydrolysis of epithelial junctional proteins by Porphyromonas gingivalis gingipains. Infect Immun. 2002;70(5):2512-8.
33. Takeuchi H, Sasaki N, Yamaga S, Kuboniwa M, Matsusaki M, Amano A. Porphyromonas gingivalis induces penetration of lipopolysaccharide and peptidoglycan through the gingival epithelium via degradation of junctional adhesion molecule 1. PLoS Pathog. 2019;15(11):e1008124.
34. Ao M, Miyauchi M, Furusho H, Inubushi T, Kitagawa M, Nagasaki A, et al. Dental Infection of Porphyromonas gingivalis Induces Preterm Birth in Mice. PLoS One. 2015;10(8):e0137249.
35. Mougeot JC, Stevens CB, Paster BJ, Brennan MT, Lockhart PB, Mougeot FK. Porphyromonas gingivalis is the most abundant species detected in coronary and femoral arteries. J Oral Microbiol. 2017;9(1):1281562.
36. Katz J, Chegini N, Shiverick KT, Lamont RJ. Localization of P. gingivalis in preterm delivery placenta. J Dent Res. 2009;88(6):575-8.

37. McCuaig R, Wong D, Gardiner FW, Rawlinson W, Dahlstrom JE, Robson S. Periodontal pathogens in the placenta and membranes in term and preterm birth. Placenta. 2018;68:40-3.
38. Puertas A, Magan-Fernandez A, Blanc V, Revelles L, O'Valle F, Pozo E, et al. Association of periodontitis with preterm birth and low birth weight: a comprehensive review. J Matern Fetal Neonatal Med. 2018;31(5):597-602.
39. Konishi H, Urabe S, Miyoshi H, Teraoka Y, Maki T, Furusho H, et al. Fetal Membrane Inflammation Induces Preterm Birth Via Toll-Like Receptor 2 in Mice With Chronic Gingivitis. Reprod Sci. 2019;26(7):869-78.
40. Takii R, Kadowaki T, Tsukuba T, Yamamoto K. Inhibition of gingipains prevents Porphyromonas gingivalis-induced preterm birth and fetal death in pregnant mice. Eur J Pharmacol. 2018;824:48-56.
41. Imamura T. The role of gingipains in the pathogenesis of periodontal disease. J Periodontol. 2003;74(1):111-8.
42. Mysak J, Podzimek S, Sommerova P, Lyuya-Mi Y, Bartova J, Janatova T, et al. Porphyromonas gingivalis: major periodontopathic pathogen overview. J Immunol Res. 2014;2014:476068.
43. Rafiei M, Kiani F, Sayehmiri F, Sayehmiri K, Sheikhi A, Zamanian Azodi M. Study of Porphyromonas gingivalis in periodontal diseases: A systematic review and meta-analysis. Med J Islam Repub Iran. 2017;31:62.
44. Bedi GS, Williams T. Purification and characterization of a collagen-degrading protease from Porphyromonas gingivalis. J Biol Chem. 1994;269(1):599-606.
45. Potempa J, Sroka A, Imamura T, Travis J. Gingipains, the major cysteine proteinases and virulence factors of Porphyromonas gingivalis: structure, function and assembly of multidomain protein complexes. Curr Protein Pept Sci. 2003;4(6):397-407.
46. Zhou J, Windsor LJ. Porphyromonas gingivalis affects host collagen degradation by affecting expression, activation, and inhibition of matrix metalloproteinases. J Periodontal Res. 2006;41(1):47-54.
47. Andrian E, Mostefaoui Y, Rouabhia M, Grenier D. Regulation of matrix metalloproteinases and tissue inhibitors of matrix metalloproteinases by Porphyromonas gingivalis in an engineered human oral mucosa model. J Cell Physiol. 2007;211(1):56-62.
48. Kadowaki T, Yoneda M, Okamoto K, Maeda K, Yamamoto K. Purification and characterization of a novel arginine-specific cysteine proteinase (argingipain) involved in the pathogenesis of periodontal disease from the culture supernatant of Porphyromonas gingivalis. J Biol Chem. 1994;269(33):21371-8.
49. Schenkein HA, Fletcher HM, Bodnar M, Macrina FL. Increased opsonization of a prtH-defective mutant of Porphyromonas gingivalis W83 is caused by reduced degradation of complement-derived opsonins. J Immunol. 1995;154(10):5331-7.
50. Jagels MA, Ember JA, Travis J, Potempa J, Pike R, Hugli TE. Cleavage of the human C5A receptor by proteinases derived from Porphyromonas gingivalis: cleavage of leukocyte C5a receptor. Adv Exp Med Biol. 1996;389:155-64.
51. Calkins CC, Platt K, Potempa J, Travis J. Inactivation of tumor necrosis factor-alpha by proteinases (gingipains) from the periodontal pathogen, Porphyromonas gingivalis. Implications of immune evasion. J Biol Chem. 1998;273(12):6611-4.
52. Darveau RP, Belton CM, Reife RA, Lamont RJ. Local chemokine paralysis, a novel pathogenic mechanism for Porphyromonas gingivalis. Infect Immun. 1998;66(4):1660-5.
53. Scott CF, Whitaker EJ, Hammond BF, Colman RW. Purification and characterization of a potent 70-kDa thiol lysyl-proteinase (Lys-gingivain) from Porphyromonas gingivalis that cleaves kininogens and fibrinogen. J Biol Chem. 1993;268(11):7935-42.
54. Grenier D. Inactivation of human serum bactericidal activity by a trypsinlike protease isolated from Porphyromonas gingivalis. Infect Immun. 1992;60(5):1854-7.
55. Carlisle MD, Srikantha RN, Brogden KA. Degradation of human alpha- and beta-defensins by culture supernatants of Porphyromonas gingivalis strain 381. J Innate Immun. 2009;1(2):118-22.

56. Cauci S, Monte R, Driussi S, Lanzafame P, Quadrifoglio F. Impairment of the mucosal immune system: IgA and IgM cleavage detected in vaginal washings of a subgroup of patients with bacterial vaginosis. J Infect Dis. 1998;178(6):1698-706.
57. Lewis WG, Robinson LS, Perry J, Bick JL, Peipert JF, Allsworth JE, et al. Hydrolysis of secreted sialoglycoprotein immunoglobulin A (IgA) in ex vivo and biochemical models of bacterial vaginosis. J Biol Chem. 2012;287(3):2079-89.
58. Borgdorff H, Gautam R, Armstrong SD, Xia D, Ndayisaba GF, van Teijlingen NH, et al. Cervicovaginal microbiome dysbiosis is associated with proteome changes related to alterations of the cervicovaginal mucosal barrier. Mucosal Immunol. 2016;9(3):621-33.
59. Doust R, Mobarez, AM. Collagenase activity in *Prevotella bivius* isolated from patients with premature rupture of membranes. Medical Journal of the Islamic Republic of Iran. 2004;18(1):61-6.
60. McGregor JA, Lawellin D, Franco-Buff A, Todd JK, Makowski EL. Protease production by microorganisms associated with reproductive tract infection. Am J Obstet Gynecol. 1986;154(1):109-14.
61. Steffen EK, Hentges DJ. Hydrolytic enzymes of anaerobic bacteria isolated from human infections. J Clin Microbiol. 1981;14(2):153-6.
62. Awano S, Ansai T, Mochizuki H, Yu W, Tanzawa K, Turner AJ, et al. Sequencing, expression and biochemical characterization of the Porphyromonas gingivalis pepO gene encoding a protein homologous to human endothelin-converting enzyme. FEBS Lett. 1999;460(1):139-44.
63. Ansai T, Yu W, Urnowey S, Barik S, Takehara T. Construction of a pepO gene-deficient mutant of Porphyromonas gingivalis: potential role of endopeptidase O in the invasion of host cells. Oral Microbiol Immunol. 2003;18(6):398-400.
64. Madeira F, Park YM, Lee J, Buso N, Gur T, Madhusoodanan N, et al. The EMBL-EBI search and sequence analysis tools APIs in 2019. Nucleic Acids Res. 2019;47(W1):W636-W41.
65. Rawlings ND, Barrett AJ, Thomas PD, Huang X, Bateman A, Finn RD. The MEROPS database of proteolytic enzymes, their substrates and inhibitors in 2017 and a comparison with peptidases in the PANTHER database. Nucleic Acids Res. 2018;46(D1):D624-D32.
66. Schomburg I, Chang A, Schomburg D. BRENDA, enzyme data and metabolic information. Nucleic Acids Res. 2002;30(1):47-9.
67. Consortium TU. UniProt: the universal protein knowledgebase in 2021. Nucleic Acids Res. 2021;49(D1).
68. Blum M, Chang HY, Chuguransky S, Grego T, Kandasaamy S, Mitchell A, et al. The InterPro protein families and domains database: 20 years on. Nucleic Acids Res. 2021;49(D1):D344-D54.
69. Almagro Armenteros JJ, Tsirigos KD, Sonderby CK, Petersen TN, Winther O, Brunak S, et al. SignalP 5.0 improves signal peptide predictions using deep neural networks. Nat Biotechnol. 2019;37(4):420-3.
70. Chen IA, Chu K, Palaniappan K, Ratner A, Huang J, Huntemann M, et al. The IMG/M data management and analysis system v.6.0: new tools and advanced capabilities. Nucleic Acids Res. 2021;49(D1):D751-D63.
71. Srinivasan S, Munch MM, Sizova MV, Fiedler TL, Kohler CM, Hoffman NG, et al. More Easily Cultivated Than Identified: Classical Isolation With Molecular Identification of Vaginal Bacteria. J Infect Dis. 2016;214 Suppl 1:S21-8.
72. McClelland RS, Lingappa JR, Srinivasan S, Kinuthia J, John-Stewart GC, Jaoko W, et al. Evaluation of the association between the concentrations of key vaginal bacteria and the increased risk of HIV acquisition in African women from five cohorts: a nested case-control study. The Lancet Infectious Diseases. 2018;18(5):554-64.
73. Parks DH, Chuvochina M, Chaumeil PA, Rinke C, Mussig AJ, Hugenholtz P. A complete domain-to-species taxonomy for Bacteria and Archaea. Nat Biotechnol. 2020;38(9):1079-86.
74. Pruesse E, Peplies J, Glockner FO. SINA: accurate high-throughput multiple sequence alignment of ribosomal RNA genes. Bioinformatics. 2012;28(14):1823-9.

75. Kumar S, Stecher G, Li M, Knyaz C, Tamura K. MEGA X: Molecular Evolutionary Genetics Analysis across Computing Platforms. Mol Biol Evol. 2018;35(6):1547-9.
76. Stamatakis A. RAxML version 8: a tool for phylogenetic analysis and post-analysis of large phylogenies. Bioinformatics. 2014;30(9):1312-3.
77. Letunic I, Bork P. Interactive Tree Of Life (iTOL) v5: an online tool for phylogenetic tree display and annotation. Nucleic Acids Research. 2021.
78. O'Flynn C, Deusch O, Darling AE, Eisen JA, Wallis C, Davis IJ, et al. Comparative Genomics of the Genus Porphyromonas Identifies Adaptations for Heme Synthesis within the Prevalent Canine Oral Species Porphyromonas cangingivalis. Genome Biol Evol. 2015;7(12):3397-413.
79. Gorasia DG, Veith PD, Chen D, Seers CA, Mitchell HA, Chen YY, et al. Porphyromonas gingivalis Type IX Secretion Substrates Are Cleaved and Modified by a Sortase-Like Mechanism. PLoS Pathog. 2015;11(9):e1005152.
80. Bauer R, Janowska K, Taylor K, Jordan B, Gann S, Janowski T, et al. Structures of three polycystic kidney disease-like domains from Clostridium histolyticum collagenases ColG and ColH. Acta Crystallogr D Biol Crystallogr. 2015;71(Pt 3):565-77.
81. Elliott SD. A Proteolytic Enzyme Produced by Group a Streptococci with Special Reference to Its Effect on the Type-Specific M Antigen. J Exp Med. 1945;81(6):573-92.
82. Matsuka YV, Pillai S, Gubba S, Musser JM, Olmsted SB. Fibrinogen cleavage by the Streptococcus pyogenes extracellular cysteine protease and generation of antibodies that inhibit enzyme proteolytic activity. Infect Immun. 1999;67(9):4326-33.
83. Nelson DC, Garbe J, Collin M. Cysteine proteinase SpeB from Streptococcus pyogenes - a potent modifier of immunologically important host and bacterial proteins. Biol Chem. 2011;392(12):1077-88.
84. Takahashi N, Kato T, Kuramitsu HK. Isolation and preliminary characterization of the Porphyromonas gingivalis prtC gene expressing collagenase activity. FEMS Microbiol Lett. 1991;68(2):135-8.
85. Kato T, Takahashi N, Kuramitsu HK. Sequence analysis and characterization of the Porphyromonas gingivalis prtC gene, which expresses a novel collagenase activity. J Bacteriol. 1992;174(12):3889-95.
86. Park Y, Yilmaz O, Jung IY, Lamont RJ. Identification of Porphyromonas gingivalis genes specifically expressed in human gingival epithelial cells by using differential display reverse transcription-PCR. Infect Immun. 2004;72(7):3752-8.
87. Wiggins R, Hicks S, Soothill P, Millar M, Corfield AJSti. Mucinases and sialidases: their role in the pathogenesis of sexually transmitted infections in the female genital tract. 2001;77(6):402-8.
88. Olmsted SS, Meyn LA, Rohan LC, Hillier SL. Glycosidase and proteinase activity of anaerobic gram-negative bacteria isolated from women with bacterial vaginosis. Sex Transm Dis. 2003;30(3):257-61.
89. Briselden AM, Moncla BJ, Stevens CE, Hillier SL. Sialidases (neuraminidases) in bacterial vaginosis and bacterial vaginosis-associated microflora. J Clin Microbiol. 1992;30(3):663-6.
90. Howe L, Wiggins R, Soothill PW, Millar MR, Horner PJ, Corfield AP. Mucinase and sialidase activity of the vaginal microflora: implications for the pathogenesis of preterm labour. Int J STD AIDS. 1999;10(7):442-7.
91. Lewis WG, Robinson LS, Gilbert NM, Perry JC, Lewis AL. Degradation, foraging, and depletion of mucus sialoglycans by the vagina-adapted Actinobacterium Gardnerella vaginalis. J Biol Chem. 2013;288(17):12067-79.
92. Wiggins R, Crowley T, Horner PJ, Soothill PW, Millar MR, Corfield AP. Use of 5-bromo-4-chloro-3-indolyl-alpha-D-N-acetylneuraminic acid in a novel spot test To identify sialidase activity in vaginal swabs from women with bacterial vaginosis. J Clin Microbiol. 2000;38(8):3096-7.

93. Moncla BJ, Braham P, Hillier SL. Sialidase (neuraminidase) activity among gram-negative anaerobic and capnophilic bacteria. J Clin Microbiol. 1990;28(3):422-5.
94. Zhang X, Xu X, Li J, Li N, Yan T, Ju X. [Relationship between vaginal sialidase bacteria vaginosis and chorioammionitis]. Zhonghua Fu Chan Ke Za Zhi. 2002;37(10):588-90.
95. Smayevsky J, Canigia LF, Lanza A, Bianchini H. Vaginal microflora associated with bacterial vaginosis in nonpregnant women: reliability of sialidase detection. Infect Dis Obstet Gynecol. 2001;9(1):17-22.
96. Sumeksri P, Koprasert C, Panichkul S. BVBLUE test for diagnosis of bacterial vaginosis in pregnant women attending antenatal care at Phramongkutklao Hospital. J Med Assoc Thai. 2005;88 Suppl 3:S7-13.
97. Myziuk L, Romanowski B, Johnson SC. BVBlue test for diagnosis of bacterial vaginosis. J Clin Microbiol. 2003;41(5):1925-8.
98. Oefner CM, Sharkey A, Gardner L, Critchley H, Oyen M, Moffett A. Collagen type IV at the fetal-maternal interface. Placenta. 2015;36(1):59-68.
99. Strauss JF, 3rd. Extracellular matrix dynamics and fetal membrane rupture. Reprod Sci. 2013;20(2):140-53.
100. Tang LJ, De Seta F, Odreman F, Venge P, Piva C, Guaschino S, et al. Proteomic analysis of human cervical-vaginal fluids. J Proteome Res. 2007;6(7):2874-83.
101. Dasari S, Pereira L, Reddy AP, Michaels JE, Lu X, Jacob T, et al. Comprehensive proteomic analysis of human cervical-vaginal fluid. J Proteome Res. 2007;6(4):1258-68.
102. Wang NY, Patras KA, Seo HS, Cavaco CK, Rosler B, Neely MN, et al. Group B streptococcal serine-rich repeat proteins promote interaction with fibrinogen and vaginal colonization. J Infect Dis. 2014;210(6):982-91.
103. Harris TO, Shelver DW, Bohnsack JF, Rubens CE. A novel streptococcal surface protease promotes virulence, resistance to opsonophagocytosis, and cleavage of human fibrinogen. J Clin Invest. 2003;111(1):61-70.
104. Katz D, Beilin Y. Disorders of coagulation in pregnancy. Br J Anaesth. 2015;115 Suppl 2:ii75-88.
105. Kadir R, Chi C, Bolton-Maggs P. Pregnancy and rare bleeding disorders. Haemophilia. 2009;15(5):990-1005.
106. Cortet M, Deneux-Tharaux C, Dupont C, Colin C, Rudigoz RC, Bouvier-Colle MH, et al. Association between fibrinogen level and severity of postpartum haemorrhage: secondary analysis of a prospective trial. Br J Anaesth. 2012;108(6):984-9.
107. Ness PM, Budzynski AZ, Olexa SA, Rodvien R. Congenital hypofibrinogenemia and recurrent placental abruption. Obstet Gynecol. 1983;61(4):519-23.
108. Evron S, Anteby SO, Brzezinsky A, Samueloff A, Eldor A. Congenital afibrinogenemia and recurrent early abortion: a case report. Eur J Obstet Gynecol Reprod Biol. 1985;19(5):307-11.
109. Goodwin TM. Congenital hypofibrinogenemia in pregnancy. Obstet Gynecol Surv. 1989;44(3):157-61.
110. Kobayashi T, Kanayama N, Tokunaga N, Asahina T, Terao T. Prenatal and peripartum management of congenital afibrinogenaemia. Br J Haematol. 2000;109(2):364-6.
111. Woessner JF, Brewer TH. Formation and Breakdown of Collagen and Elastin in the Human Uterus during Pregnancy and Post-Partum Involution. Biochem J. 1963;89:75-82.
112. Montoya TI, Maldonado PA, Acevedo JF, Word RA. Effect of vaginal or systemic estrogen on dynamics of collagen assembly in the rat vaginal wall. Biol Reprod. 2015;92(2):43.
113. Kerkhof MH, Hendriks L, Brolmann HA. Changes in connective tissue in patients with pelvic organ prolapse--a review of the current literature. Int Urogynecol J Pelvic Floor Dysfunct. 2009;20(4):461-74.

114. Minamoto T, Arai K, Hirakawa S, Nagai Y. Immunohistochemical studies on collagen types in the uterine cervix in pregnant and nonpregnant states. Am J Obstet Gynecol. 1987;156(1):138-44.
115. Myers K, Socrate S, Tzeranis D, House M. Changes in the biochemical constituents and morphologic appearance of the human cervical stroma during pregnancy. Eur J Obstet Gynecol Reprod Biol. 2009;144 Suppl 1:S82-9.
116. Myers KM, Paskaleva AP, House M, Socrate S. Mechanical and biochemical properties of human cervical tissue. Acta Biomater. 2008;4(1):104-16.
117. Uldbjerg N, Ekman G, Malmstrom A, Olsson K, Ulmsten U. Ripening of the human uterine cervix related to changes in collagen, glycosaminoglycans, and collagenolytic activity. Am J Obstet Gynecol. 1983;147(6):662-6.
118. Osmers R, Rath W, Adelmann-Grill BC, Fittkow C, Severenyi M, Kuhn W. Collagenase activity in the cervix of non-pregnant and pregnant women. Arch Gynecol Obstet. 1990;248(2):75-80.
119. Rath W, Adelmann-Grill BC, Pieper U, Kuhn W. Collagen degradation in the pregnant human cervix at term and after prostaglandin-induced cervical ripening. Arch Gynecol. 1987;240(3):177-84.
120. Gonzalez JM, Dong Z, Romero R, Girardi G. Cervical remodeling/ripening at term and preterm delivery: the same mechanism initiated by different mediators and different effector cells. PLoS One. 2011;6(11):e26877.
121. Parry S, Strauss JF, 3rd. Premature rupture of the fetal membranes. N Engl J Med. 1998;338(10):663-70.
122. Jones HE, Harris KA, Azizia M, Bank L, Carpenter B, Hartley JC, et al. Differing prevalence and diversity of bacterial species in fetal membranes from very preterm and term labor. PLoS One. 2009;4(12):e8205.
123. Wang H, Ogawa M, Wood JR, Bartolomei MS, Sammel MD, Kusanovic JP, et al. Genetic and epigenetic mechanisms combine to control MMP1 expression and its association with preterm premature rupture of membranes. Hum Mol Genet. 2008;17(8):1087-96.
124. McLaren J, Taylor DJ, Bell SC. Increased concentration of pro-matrix metalloproteinase 9 in term fetal membranes overlying the cervix before labor: implications for membrane remodeling and rupture. Am J Obstet Gynecol. 2000;182(2):409-16.
125. Skinner SJ, Campos GA, Liggins GC. Collagen content of human amniotic membranes: effect of gestation length and premature rupture. Obstet Gynecol. 1981;57(4):487-9.
126. McGregor JA, French JI, Lawellin D, Franco-Buff A, Smith C, Todd JK. Bacterial protease-induced reduction of chorioamniotic membrane strength and elasticity. Obstet Gynecol. 1987;69(2):167-74.
127. Chopra A, Radhakrishnan R, Sharma M. Porphyromonas gingivalis and adverse pregnancy outcomes: a review on its intricate pathogenic mechanisms. Crit Rev Microbiol. 2020;46(2):213-36.
128. Wu YM, Chen LL, Yan J, Zhuang CY, Gu ZY. Effect of Porphyromonas gingivalis PrtC on cytokine expression in ECV304 endothelial cells and its level in subgingival plaques from patients with chronic periodontitis. Acta Pharmacol Sin. 2007;28(7):1015-23.
129. Houle MA, Grenier D, Plamondon P, Nakayama K. The collagenase activity of Porphyromonas gingivalis is due to Arg-gingipain. FEMS Microbiol Lett. 2003;221(2):181-5.
130. Kuramitsu HK, Yoneda M, Madden T. Proteases and collagenases of Porphyromonas gingivalis. Adv Dent Res. 1995;9(1):37-40.
131. Bhattacharya S, Bhattacharya S, Gachhui R, Hazra S, Mukherjee J. U32 collagenase from Pseudoalteromonas agarivorans NW4327: Activity, structure, substrate interactions and molecular dynamics simulations. Int J Biol Macromol. 2019;124:635-50.
132. Wu Q, Li C, Li C, Chen H, Shuliang L. Purification and characterization of a novel collagenase from Bacillus pumilus Col-J. Appl Biochem Biotechnol. 2010;160(1):129-39.
133. Filep JG. Endothelin peptides: biological actions and pathophysiological significance in the lung. Life Sci. 1993;52(2):119-33.

134. Noveral JP, Rosenberg SM, Anbar RA, Pawlowski NA, Grunstein MM. Role of endothelin-1 in regulating proliferation of cultured rabbit airway smooth muscle cells. Am J Physiol. 1992;263(3 Pt 1):L317-24.
135. Pritchard GG, Freebairn AD, Coolbear T. Purification and characterization of an endopeptidase from Lactococcus lactis subsp. cremoris SK11. Microbiology (Reading). 1994;140 (Pt 4):923-30.
136. Christensson C, Bratt H, Collins LJ, Coolbear T, Holland R, Lubbers MW, et al. Cloning and expression of an oligopeptidase, PepO, with novel specificity from Lactobacillus rhamnosus HN001 (DR20). Appl Environ Microbiol. 2002;68(1):254-62.
137. Agarwal V, Kuchipudi A, Fulde M, Riesbeck K, Bergmann S, Blom AM. Streptococcus pneumoniae endopeptidase O (PepO) is a multifunctional plasminogen- and fibronectin-binding protein, facilitating evasion of innate immunity and invasion of host cells. J Biol Chem. 2013;288(10):6849-63.
138. Agarwal V, Sroka M, Fulde M, Bergmann S, Riesbeck K, Blom AM. Binding of Streptococcus pneumoniae endopeptidase O (PepO) to complement component C1q modulates the complement attack and promotes host cell adherence. J Biol Chem. 2014;289(22):15833-44.
139. Shu Z, Yuan J, Wang H, Zhang J, Li S, Zhang H, et al. Streptococcus pneumoniae PepO promotes host anti-infection defense via autophagy in a Toll-like receptor 2/4 dependent manner. Virulence. 2020;11(1):270-82.
140. Zhang H, Kang L, Yao H, He Y, Wang X, Xu W, et al. Streptococcus pneumoniae Endopeptidase O (PepO) Elicits a Strong Innate Immune Response in Mice via TLR2 and TLR4 Signaling Pathways. Front Cell Infect Microbiol. 2016;6:23.
141. Wilkening RV, Chang JC, Federle MJ. PepO, a CovRS-controlled endopeptidase, disrupts Streptococcus pyogenes quorum sensing. Mol Microbiol. 2016;99(1):71-87.
142. Honda-Ogawa M, Sumitomo T, Mori Y, Hamd DT, Ogawa T, Yamaguchi M, et al. Streptococcus pyogenes Endopeptidase O Contributes to Evasion from Complement-mediated Bacteriolysis via Binding to Human Complement Factor C1q. J Biol Chem. 2017;292(10):4244-54.